

Accepted Manuscript

Synthesis and photocytotoxic activity of [1,2,3]triazolo[4,5-*h*][1,6]naphthyridines and [1,3]oxazolo[5,4-*h*][1,6]naphthyridines

Ilaria Frasson, Virginia Spanò, Simona Di Martino, Matteo Nadai, Filippo Doria, Barbara Parrino, Anna Carbone, Stella Maria Cascioferro, Patrizia Diana, Girolamo Cirrincione, Mauro Freccero, Paola Barraja, Sara N. Richter, Alessandra Montalbano

PII: S0223-5234(18)30948-6

DOI: <https://doi.org/10.1016/j.ejmech.2018.10.071>

Reference: EJMECH 10857

To appear in: *European Journal of Medicinal Chemistry*

Received Date: 31 May 2018

Revised Date: 2 October 2018

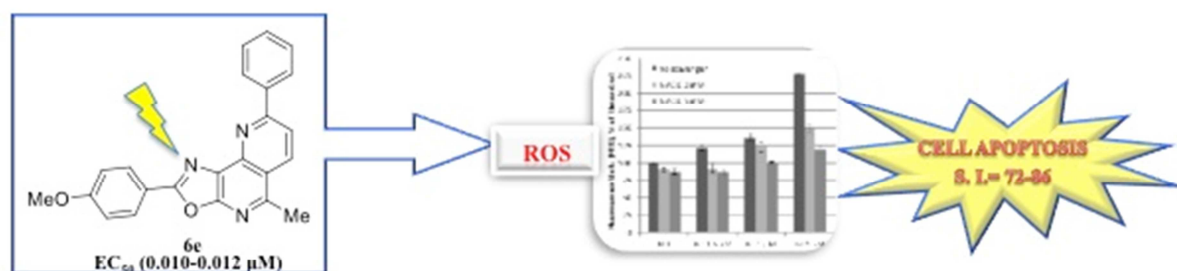
Accepted Date: 31 October 2018

Please cite this article as: I. Frasson, V. Spanò, S. Di Martino, M. Nadai, F. Doria, B. Parrino, A. Carbone, S.M. Cascioferro, P. Diana, G. Cirrincione, M. Freccero, P. Barraja, S.N. Richter, A. Montalbano, Synthesis and photocytotoxic activity of [1,2,3]triazolo[4,5-*h*][1,6]naphthyridines and [1,3]oxazolo[5,4-*h*][1,6]naphthyridines, *European Journal of Medicinal Chemistry* (2018), doi: <https://doi.org/10.1016/j.ejmech.2018.10.071>.

This is a PDF file of an unedited manuscript that has been accepted for publication. As a service to our customers we are providing this early version of the manuscript. The manuscript will undergo copyediting, typesetting, and review of the resulting proof before it is published in its final form. Please note that during the production process errors may be discovered which could affect the content, and all legal disclaimers that apply to the journal pertain.



Graphical abstract



Synthesis and photocytotoxic activity of [1,2,3]triazolo[4,5-*h*][1,6]naphthyridines and [1,3]oxazolo[5,4-*h*][1,6]naphthyridines

Ilaria Frasson^{a,1}, Virginia Spanò^{b,1}, Simona Di Martino^b, Matteo Nadai^a,
Filippo Doria^c, Barbara Parrino^b, Anna Carbone^b, Stella Maria Cascioferro^b,
Patrizia Diana^b, Girolamo Cirrincione^b, Mauro Freccero^c, Paola Barraja^b,
Sara N. Richter^{a*}, Alessandra Montalbano^{b*}

^a Dipartimento di Medicina Molecolare, Università degli Studi di Padova, Via Gabelli 63, 35121 Padova, Italy; ^b Dipartimento di Scienze e Tecnologie Biologiche Chimiche e Farmaceutiche (STEBICEF), Università degli Studi di Palermo, Via Archirafi 32, 90123 Palermo, Italy; ^c Dipartimento di Chimica, Università degli Studi di Pavia, Viale Taramelli 10, 27100 Pavia, Italy.

¹ The authors contributed equally to this work.

ABSTRACT [1,2,3]Triazolo[4,5-*h*][1,6]naphthyridines and [1,3]oxazolo[5,4-*h*][1,6]naphthyridines were synthesized with the aim to investigate their photocytotoxic activity. Upon irradiation, oxazolo-naphthyridines induced light-dependent cell death at nanomolar/low micromolar concentrations (EC₅₀ 0.01–6.59 μM). The most photocytotoxic derivative showed very high selectivity and photocytotoxicity indexes (SI=72-86, PTI>5000), along with a triplet excited state with exceptionally long lifetime (18.0 μs) and high molar absorptivity (29781±180 M⁻¹cm⁻¹ at λ_{max} 315 nm). The light-induced production of ROS promptly induced an unquenchable apoptotic process selectively in tumor cells, with mitochondrial and lysosomal

involvement. Altogether, these results demonstrate that the most active compound acts as a promising singlet oxygen sensitizer for biological applications.

KEYWORDS: [1,2,3]Triazolo[4,5-*h*][1,6]naphthyridines, [1,3]oxazolo[5,4-*h*][1,6]naphthyridines, photochemiotherapy, photosensitizing agents, reactive oxygen species.

1. Introduction

Naphthyridines (also known as pyridopyridines or diazanaphthalenes) are nitrogen heterocyclic compounds widely used in agriculture, in analytical chemistry, in diagnostics and for the treatment of different human diseases. [1]

Among the six possible isomers (1,5-, 1,6-, 1,7-, 1,8- 2,6- and 2,7-pyridopyridines), [1,6]naphthyridines are endowed with interesting biological properties including antibacterial, [2, 3] and anticonvulsant activity. [4] They have also been used as potent antiviral agents against both the human cytomegalovirus (HCMV) [5-7] and human immunodeficiency virus-1 (HIV-1). In fact, 8-hydroxy[1,6]naphthyridines **1** and **2** (Chart 1) proved to reduce HIV-1 integrase activity and to inhibit 95% of the spread of viral infection in cell culture at 0.39 μM and 18.6 nM respectively. [8,9] Further studies revealed that new derivatives of type **3**, obtained from modification of the decoration of the lead structure at the 8-position, were endowed with significant cytotoxicity against a panel of cancer cell lines and inhibited selected oncogenic kinases. [10] FGFR-1 and VEGFR-2 kinases inhibitory activities at low nanomolar level were also exhibited by 7-acetamido[1,6]naphthyridines (**4**) synthesized by Thompson et al. [11,12]

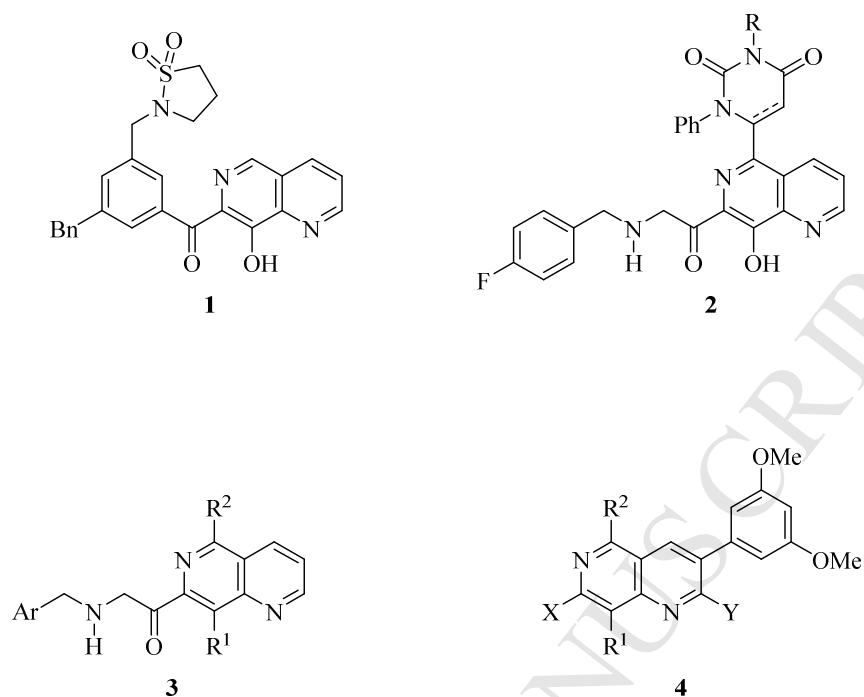


Chart 1. Structures of [1,6]naphthyridine derivatives **1-4**.

Thus, considering the interesting properties showed by the [1,6]naphthyridine scaffold we synthesized tricyclic systems of type **5-8** (Chart 2) in which the triazole or oxazole moieties are annelated to the diazabicyclic portion. These new ring systems can be also regarded as hetero-analogues of quinolines of type **9** and **10**, potent photosensitizers previously reported by us, containing a pyrrole and a pyrazole ring respectively. [13-16] In particular, one class of pyrroloquinolones (**9**), upon light activation at a proper wavelength, showed potent growth inhibitory activity at submicromolar level (0.5-7.2 μM). Cellular photocytotoxicity was related to production of reactive oxygen species (ROS) with the involvement of both mitochondria and lysosomes, alteration of the cell cycle profile and membrane lipid peroxidation, without DNA photodamage. Condensation of the quinoline moiety to the pyrazole ring, led to pyrazolo[3,4-*h*]quinolines (**10**); this structural modification led to the improvement of photocytotoxicity with

growth inhibition of 50% of the cell population (GI_{50}) reaching nanomolar level (0.04-14.52 μM). Derivatives **10** were able to generate high levels of superoxide anion and singlet oxygen, suggesting involvement of both type I and type II oxygen-dependent photosensitization mechanisms. [16]

More recently we have studied pyrrolo[3',2':6,7]cyclohepta[1,2-*d*]pyrimidines (**11**) and pyrrolo[3',2':6,7]cyclohepta[1,2-*b*]pyridines (**12**) which showed very promising antitumor properties. [17,18] Upon photoactivation with light of the proper wavelength, they showed cytotoxic effect at 0.06–4.96 μM and 0.19–10.70 μM respectively, inducing apoptosis associated with rapid and massive production of large amounts of ROS, mitochondrial morphology modifications and activation of lysosomes. Unfortunately, although these two classes of derivatives were endowed with potent photocytotoxic activity, they were not very selective for tumor cell lines.

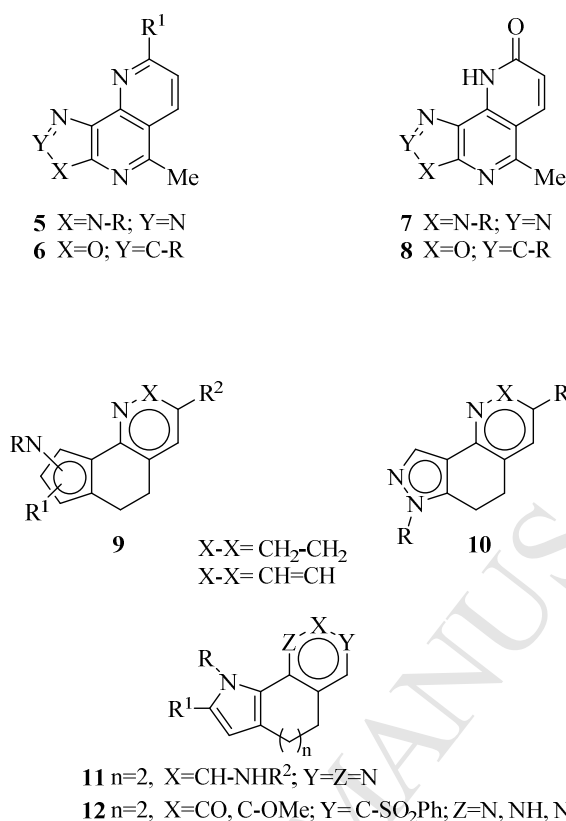


Chart 2. Structures of [1,2,3]triazolo[4,5-*h*][1,6]naphthyridines (**5**, **7**), [1,3]oxazolo[5,4-*h*][1,6]naphthyridines (**6**, **8**), pyrroloquinolines (**9**), pyrazoloquinolines (**10**), pyrrolo[3',2':6,7]cyclohepta[1,2-*d*]pyrimidines (**11**) and pyrrolo[3',2':6,7]cyclohepta[1,2-*b*]pyridines (**12**).

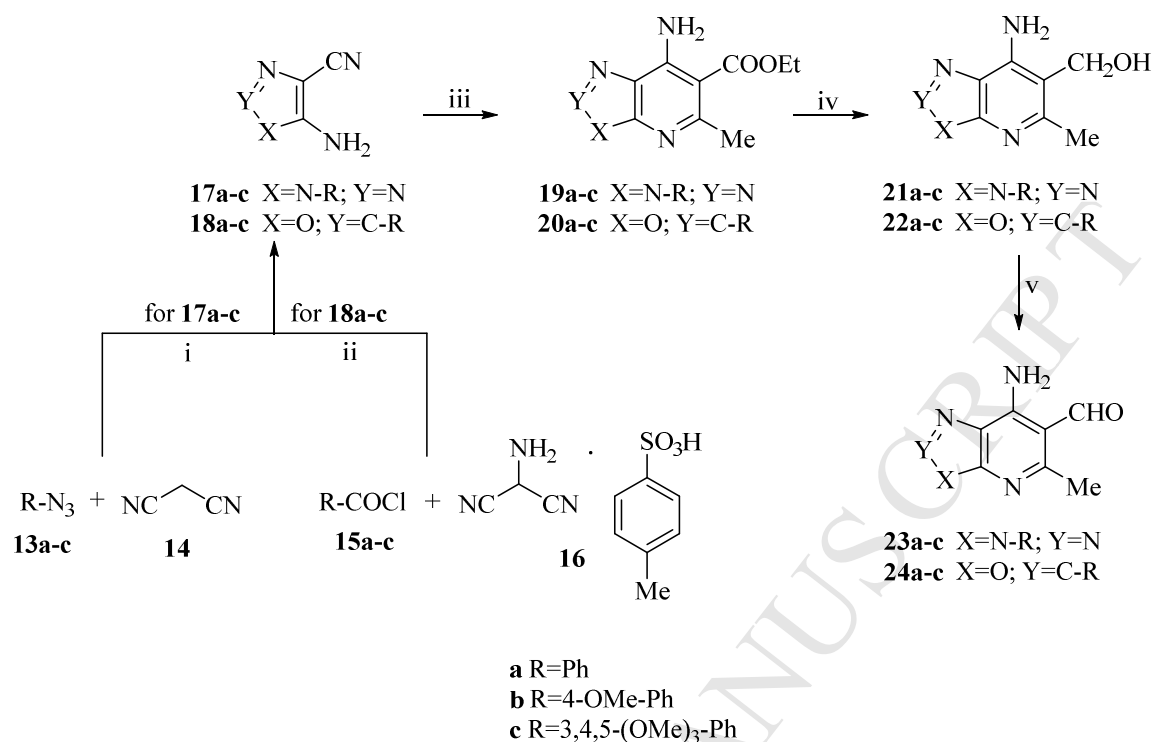
Thus, as part of our search for nitrogen heterocycles [19-37] and considering that the antitumor effect of [1,6]naphthyridines has been widely investigated, but no examples of their photochemotherapeutic activity have been reported so far, herein we report the synthesis of the new ring systems [1,2,3]triazolo[4,5-*h*][1,6]naphthyridines **5a-l**, **7a-c**, and [1,3]oxazolo[5,4-*h*][1,6]naphthyridines **6a-l**, **8a-c** with the aim of investigating their antiproliferative effect either in the dark and under light irradiation.

2. Results and Discussion

2.1. Chemistry

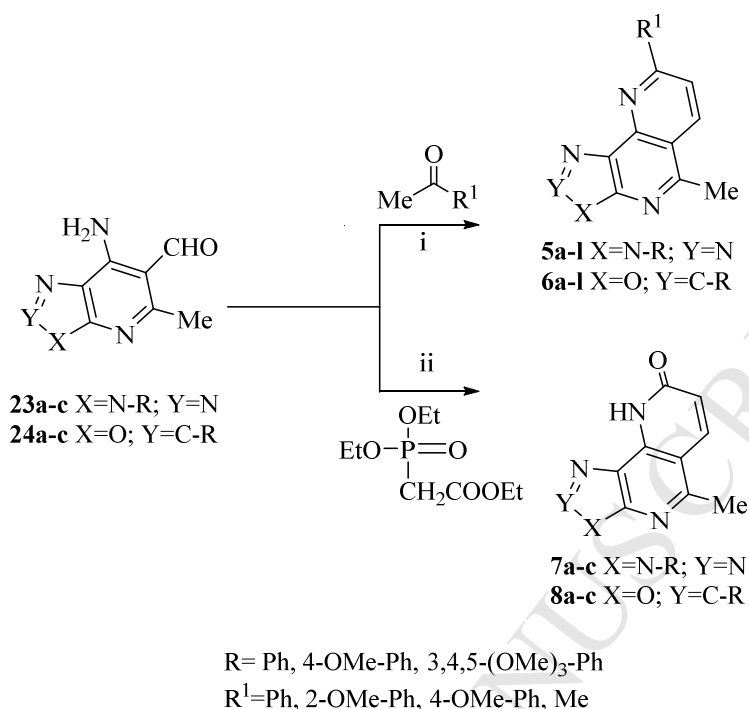
The key intermediates 7-amino-5-methyl-3-substituted-3*H*-[1,2,3]triazolo[4,5-*b*]pyridine-6-carbaldehydes (**23a-c**) and 7-amino-5-methyl-2-substituted-[1,3]oxazolo[5,4-*b*]pyridine-6-carbaldehydes (**24a-c**) were prepared starting from the suitable 5-amino-1-substituted-1*H*-1,2,3-triazole-4-carbonitrile derivatives (**17a-c**) or 5-amino-2-substituted-[1,3]oxazole-4-carbonitrile derivatives (**18a-c**) respectively (Scheme 1).

In particular, compounds **17a-c** were obtained through a 1,3-dipolar cycloaddition of the proper azido-derivatives (**13a-c**) with malononitrile (**14**) in the presence of sodium ethoxide. 5-Amino-2-substituted-[1,3]oxazole-4-carbonitrile derivatives **18a-c** were prepared through the van Leusen oxazole synthesis, according to the general method reported by Freeman and Kim. [38] Thus a solution of commercially available aminomalnonitrile tosylate (**16**) in 1-methyl-2-pyrrolidone was reacted with the proper benzoyl chloride (**15a-c**). The desired compounds **17a-c** and **18a-c** were subsequently refluxed with ethyl acetoacetate, in the presence of stannic chloride as strong Lewis acid, allowing the isolation of 7-amino-5-methyl-3-substituted-3*H*-[1,2,3]triazolo[4,5-*b*]pyridine-6-carboxylate derivatives (**19a-c**) and ethyl 7-amino-5-methyl-2-substituted[1,3]oxazolo[5,4-*b*]pyridine-6-carboxylates (**20a-c**). These latter were subjected to reduction of the ethoxycarbonyl group with lithium aluminium hydride in THF to give compounds **21a-c** and **22a-c**, which were in turn submitted to oxidation reaction with Dess-Martin periodinane in dichloromethane, leading to the corresponding key intermediate *o*-aminoaldehydes **23a-c** and **24a-c** which were used without further purification.



Scheme 1. Synthesis of key intermediates **23a-c**, and **24a-c**.

Reagents: (i) EtONa, ethanol, 0 °C-rt, 12 h, 60-70%; (ii) 1-methyl-2-pyrrolidinone, rt, 12 h, 51-79%; (iii) ethyl acetoacetate, toluene, stannic chloride, reflux, 4 h, 45-62% (for derivatives **19a-c**), 45-65% (for derivatives **20a-c**); (iv) LiAlH₄, THF, 0 °C-rt, 12 h, 58-92% (for derivatives **21a-c**), 55-80% (for derivatives **22a-c**); (v) Dess-Martin periodinane, DCM, rt, 5 h.

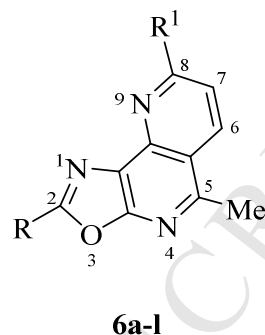
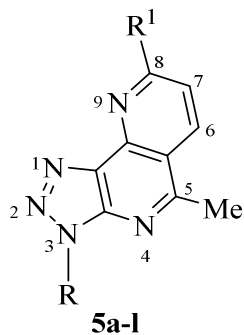


Scheme 2. Synthesis of naphthyridine derivatives **5a-l**, **6a-l** and naphthyridine-8-one derivatives **7a-c**, **8a-c**.

Reagents: (i) KOH, ethanol and suitable ketone, or KOH and acetone (for derivatives **5d**, **5h**, **5l**, **6d**, **6h**, **6l**) reflux, 12 h, 42-65% (for derivatives **5a-l**), 40-58% (for derivatives **6a-l**); (ii) K₂CO₃, ethanol, reflux, 12 h, 40-60% (for derivatives **7a-c**), 45-62% (for derivatives **8a-c**).

Cyclization to naphthyridine derivatives **5a-l** and **6a-l** was achieved through Friendlander condensation of compounds **23a-c** and **24a-c**, respectively, with acetophenone or substituted acetophenones, such as 2-methoxy-acetophenone, 4-methoxy-acetophenone and acetone, in basic media (Table 1).

Table 1. Naphthyridine derivatives **5a-l** and **6a-l** and spectrophotometric properties of selected naphthyridine derivatives of type **5, 6**.



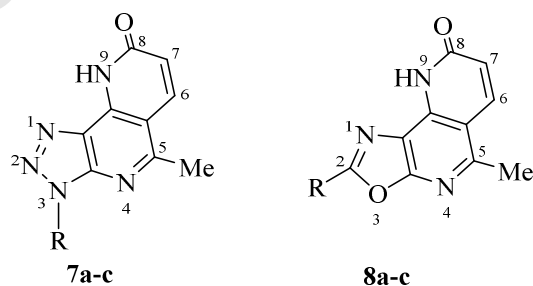
Compd	R	R ¹	λ_{\max} (nm)	ϵ_{\max}	ϵ_{365} (nm)
5a	Ph	Ph	337	9200	6624
5b	Ph	2-OMe-Ph	-	-	-
5c	Ph	4-OMe-Ph	365	8188	8188
5d	Ph	Me	310	5200	80
5e	4-OMe-Ph	Ph	-	-	-
5f	4-OMe-Ph	2-OMe-Ph	354	5600	5148
5g	4-OMe-Ph	4-OMe-Ph	351	6400	6352
5h	4-OMe-Ph	Me	302	3520	2316
5i	3,4,5-(OMe) ₃ -Ph	Ph	334	5200	3560
5j	3,4,5-(OMe) ₃ -Ph	2-OMe-Ph	352	11600	11172
5k	3,4,5-(OMe) ₃ -Ph	4-OMe-Ph	-	-	-
5l	3,4,5-(OMe) ₃ -Ph	Me	-	-	-
6a	Ph	Ph	-	-	-
6b	Ph	2-OMe-Ph	360	11428	11224
6c	Ph	4-OMe-Ph	-	-	-
6d	Ph	Me	338	10632	2396

6e	4-OMe-Ph	Ph	325	21760	15384
6f	4-OMe-Ph	2-OMe-Ph	-	-	-
6g	4-OMe-Ph	4-OMe-Ph	-	-	-
6h	4-OMe-Ph	Me	350	10588	7588
6i	3,4,5-(OMe) ₃ -Ph	Ph	330	15780	11800
6j	3,4,5-(OMe) ₃ -Ph	2-OMe-Ph	327	9976	9084
6k	3,4,5-(OMe) ₃ -Ph	4-OMe-Ph	-	-	-
6l	3,4,5-(OMe) ₃ -Ph	Me	300	13940	5688

The absorption spectra were collected in 20 mM phosphate buffer (PB), pH 7.4 and ϵ were calculated.

Alternatively, *o*-aminoaldehydes **23a-c** and **24a-c** were reacted with triethyl phosphonoacetate, using potassium carbonate as base, allowing the isolation of naphthyridine-8-ones derivatives **7a-c** and **8a-c** (Table 2).

Table 2. Naphthyridine-8-one derivatives **7a-c** and **8a-c** and spectrophotometric properties of selected naphthyridine-8-one derivatives of type **7**, **8**.



Compd	R	λ_{\max} (nm)	ϵ_{\max}	ϵ_{365} (nm)
7a	Ph	325	8000	924
7b	4-OMe-Ph	325	5600	3476
7c	3,4,5-(OMe) ₃ -Ph	-	-	-
8a	Ph	300	21188	176
8b	4-OMe-Ph	-	-	-
8c	3,4,5-(OMe) ₃ -Ph	-	-	-

The absorption spectra were collected in 20 mM phosphate buffer (PB), pH 7.4 and ϵ were calculated.

2.2 Biology

2.2.1 Spectrophotometric properties

The essential requirement for a photosensitizer compound is the absorption of UV-Vis light. The absorption spectra of compounds were collected in phosphate buffer (20 mM, pH 7.4) and ϵ values were calculated in correspondence of both λ_{\max} and $\lambda_{365 \text{ nm}}$. All compounds absorbed UV-Vis light with maximum peaks in the UV-A region (300-365 nm), a fundamental feature for a photosensitizer (Tables 1, 2 and Figure S1).

2.2.2 Antiproliferative assays

The antiproliferative activity of the tested compounds was evaluated on a panel of cultured human tumor cell lines, representing the most common neoplasms: MCF7 (mammary gland adenocarcinoma), HT-29 (colorectal adenocarcinoma) and A375 (malignant melanoma) cells. Besides tumor cell lines, the compounds were tested also on the non-tumor cell line MCF10A (mammary gland epithelial cells) to assess their selectivity towards malignancies. Moreover, the

antiproliferative experiments were performed without irradiation by incubating cells with compounds for 72 h to evaluate the UV light-independent cytotoxicity.

Prior to the administration of the compounds, all cell lines were tested for UV phototoxicity to achieve the highest compounds' activation in the absence of cellular cytotoxicity. We set up a light dose of 1.5 J/cm^2 (corresponding to 5 min of light exposure at 365 nm) at which the amount of living cells in the UV-treated and UV-untreated samples was the same. Phototoxicity was assessed by MTT test 72 h after UV irradiation in the presence of the compounds. [17,18] Phototoxicity was evaluated only for compounds with adequate solubility in DMSO and reported as the effective concentration able to kill 50% of the cell population (EC_{50} , Table 3, Figure S2 for photocytotoxicity curves of most active compounds); toxicity in the absence of UV exposure was indicated as the cytotoxic concentration able to kill 50% of the cell population (CC_{50}).

Table 3. Photocytotoxicity EC_{50} (μM) and cytotoxicity CC_{50} (μM) in human tumor and non-tumor cell lines measured 72 h post administration of selected naphthyridine derivatives of type **5**, **6** and naphthyridine-8-one derivatives of type **7**, **8**.

Compd	Human cell lines											
	A375			HT-29			MCF7			MCF10A		
	^a EC_{50} (μM)	^b CC_{50} (μM)	^c PTI	EC_{50} (μM)	CC_{50} (μM)	PTI	EC_{50} (μM)	CC_{50} (μM)	PTI	EC_{50} (μM)	CC_{50} (μM)	PTI
5a	>50±0	>50±0	n.d.	>50±0	>50±0	n.d.	>50±0	>50±0	n.d.	>50±0	>50±0	n.d.
5c	10.100±6.920	>50±0	>5	0.099±0.017	>50±0	>508	33.958±12.600	>50±0	>1.5	0.099±0.009	>50±0	>505
5d	>50±0	>50±0	n.d.	>50±0	>50±0	n.d.	>50±0	>50±0	n.d.	>50±0	>50±0	n.d.
5f	1.094±0.033	>50±0	>46	>50±0	>50±0	n.d.	>50±0	>50±0	n.d.	>50±0	>50±0	n.d.
5g	0.875±0.031	>50±0	>57	1.735±0.870	>50±0	>29	>50±0	>50±0	n.d.	>50±0	>50±0	n.d.
5h	>50±0	>50±0	n.d.	>50±0	>50±0	n.d.	>50±0	>50±0	n.d.	>50±0	>50±0	n.d.
5i	>50±0	>50±0	n.d.	>50±0	>50±0	n.d.	>50±0	>50±0	n.d.	>50±0	>50±0	n.d.
5j	>50±0	>50±0	n.d.	>50±0	>50±0	n.d.	>50±0	>50±0	n.d.	>50±0	>50±0	n.d.
6b	0.633±0.081	>50±0	>79	0.197±0.067	>50±0	>254	1.323±0.371	>50±0	>38	1.170±0.099	>50±0	>43
6d	>50±0	>50±0	n.d.	6.587±0.158	>50±0	>8	>50±0	>50±0	n.d.	>50±0	>50±0	n.d.
6e	0.011±0.009	>50±0	>4545	0.012±0.002	>50±0	>4167	0.010±0.008	>50±0	>5000	0.864±0.150	>50±0	>58
6h	>50±0	>50±0	n.d.	4.283±0.339	>50±0	>12	>50±0	>50±0	n.d.	>50±0	>50±0	n.d.

6i	1.441±0.600	>50±0	>35	0.620±0.069	>50±0	>81	5.944±0.301	>50±0	>8	4.380±0.099	>50±0	>11
6j	0.764±0.034	>50±0	>65	0.197±0.020	>50±0	>254	3.529±0.226	>50±0	>14	1.860±0.086	>50±0	>27
6l	>50±0	>50±0	n.d.									
7a	>50±0	>50±0	n.d.									
7b	>50±0	>50±0	n.d.									
8a	1.490±0.035	>50±0	>34	>50±0	>50±0	n.d.	>50±0	>50±0	n.d.	>50±0	>50±0	n.d.

Data are expressed as mean \pm SD of at least three different independent experiments. ^a EC₅₀: Photocytotoxic concentration able to kill 50% of the cell population. ^b CC₅₀: Cytotoxic concentration able to kill 50% of the cell population. ^c PTI: Phototoxic index corresponds to CC₅₀/EC₅₀ ratio; it indicates the effectiveness of the tested compounds upon photoactivation. n.d.: not determined.

The CC_{50}/EC_{50} ratio was defined as the photoactivation toxicity index (PTI), i.e. the compounds' ability to kill cells only upon light activation. Moreover, the selectivity index (SI), expressed as EC_{50} of the photoactivated compound in the *normal* cell line/ EC_{50} of the same compound in the *cancer* cell line, was assessed (Table 4).

Notably, no cytotoxicity was observed in all the three cell lines by MTT analysis after 72 h of incubation with up to 50 μM of the compounds in the absence of UV-light exposure (Table 3).

Although clear-cut structure-activity relationships (SAR) are not easily assessed, some hypotheses can be formulated. Comparing the two classes of compounds, triazole derivatives **5** and **7** displayed lower cytotoxicity and tumor selectivity, compared to oxazolo-naphthyridines **6** and naphthyridine-8-ones **8**. Triazolo-naphthyridines, of which only three derivatives (**5c**, **5f** and **5g**) out of the eight could be screened, demonstrated photocytotoxicity with EC_{50} values at the submicromolar/micromolar level (EC_{50} 0.099–33.958 μM); in particular they showed high cytotoxicity on the A375 cell line, with EC_{50} values from submicromolar (**5g**: EC_{50} 0.875 μM) to micromolar (**5c**: EC_{50} 10.100 μM , Figure S2). The latter derivative **5c** was the only one, among the three, which proved to be photocytotoxic also against HT-29 (EC_{50} 0.099 μM) and MCF7 cell line (EC_{50} 33.958 μM) and displayed antiproliferative activity also against the non-tumor cell line MCF10A. In contrast, triazolo-naphthyridine-8-ones **7a** and **7b** were not cytotoxic against the three tested tumor cell lines, likely because of their low molar extinction coefficient at 365 nm.

The best results were obtained with oxazolo-naphthyridines **6**: upon irradiation, four out of seven tested derivatives were able to induce UV dependent cell death at nanomolar/low micromolar concentrations (EC_{50} 0.010–6.587 μM). The most potent derivative was **6e** (EC_{50} 0.010–0.012 μM , Figure S2), which bears a 4-methoxy-phenyl group at position 2 and a phenyl ring at

position 8. Replacement of the phenyl ring with a methyl group in position 8 caused a drastic loss of activity (compare **6e** with **6h**). Moreover, removal of 4-methoxy-phenyl group and its substitution with a phenyl (**6b**) or 3,4,5-trimethoxyphenyl group (**6i**, **6j**) decreased phototoxicity (**6b**: EC₅₀ 0.197–1.323 μM, **6i**: EC₅₀ 0.620–5.944 μM, **6j**: EC₅₀ 0.197–3.529 μM). In the 3,4,5-trimethoxy series, the methyl group in position 8 caused again a complete loss of phototoxicity (**6l**).

Oxazolo-naphthyridine-8-one derivative **8a** expressed photocytotoxicity at low micromolar level only against the A375 cell line (EC₅₀ 1.490 μM).

Crucial requirements for photosensitizing agents are photocytotoxicity coupled to high ϵ and SI values; the most photocytotoxic compound **6e** fulfils these features. It induced UV-dependent cell death at nanomolar concentrations, the same order of magnitude of pyrrolo[3',2':6,7]cyclohepta[1,2-*d*]pyrimidines **11**, ROS-inducer photosensitizers previously reported by us (EC₅₀ 0.06–4.96 μM), [17] but in comparison with these, **6e** is endowed with much higher CC₅₀/EC₅₀ ratio (PTI >5000 in MCF7 cell line) and selectivity for the tumor cell lines (SI 72-86) (Table 4). Interestingly **6e** is very active on the MCF7 cell line (breast cancer), which is one of the most studied human breast cancer cell line and usually not very sensitive to drugs. [39,40] When compared to other published PS, such as zinc Phthalocyanine, **6e** demonstrated no cytotoxicity in the absence of irradiation and much lower EC₅₀ (nanomolar vs micromolar range) than phthalocyanine on tumor cell lines. [41] Moreover, taking into consideration compounds with similar absorption spectra and intracellular accumulation, i.e. Chlorine e₆ and derivatives, **6e** was characterized by a higher cytotoxic effect (EC₅₀ in the low nanomolar range vs micromolar-high nanomolar range of Chlorine e₆ and derivatives) and a

remarkably higher PTI (>5000 for **6e** vs 466.6 of the most active Chlorine e₆ derivatives). [42]

These are very promising results, which pave the way to further drug development.

Table 4. SI values of selected naphthyridine derivatives of type **5-6** and of naphthyridine-8-one derivatives of type **7-8**.

Compd	MCF10A/A375	MCF10A/HT-29	MCF10A/MCF7
5a	n.d.	n.d.	n.d.
5c	0.009	1.01	0.003
5d	n.d.	n.d.	n.d.
5f	46	>1	>1
5g	57	29	>1
5h	n.d.	n.d.	n.d.
5i	n.d.	n.d.	n.d.
5j	n.d.	n.d.	n.d.
6b	2	6	0.884
6d	n.d.	8	n.d.
6e	79	72	86
6h	n.d.	12	n.d.
6i	3	7	0.737
6j	2	9	0.527
6l	n.d.	n.d.	n.d.
7a	n.d.	n.d.	n.d.
7b	n.d.	n.d.	n.d.
8a	34	n.d.	n.d.

SI: selectivity index corresponds to EC_{50} of photoactivated compound in the *normal* cell line/ EC_{50} of the same compound in the *cancer* cell line and indicates the degree of tumor selectivity of the photoactivated compounds.

2.2.3 Cell cytotoxicity localization: cytosolic ROS induction is required for naphthyridines-induced cell death

To explore the cellular mechanisms underlying phototoxicity of the tested compounds, we chose the most active and selective compound (**6e**) for further biological assays. To assess the cellular compartments affected by the compound, we administrated **6e** to MCF7 cells and monitored its localization over 1 h time (Figure 1 and Figure S3), taking advantage of the residual fluorescence (Figure S4). In fact, **6e** exhibited a maximum in the fluorescent emission at 468 nm with a non-negligible fluorescent quantum yield ($\Phi_F = 0.2$).

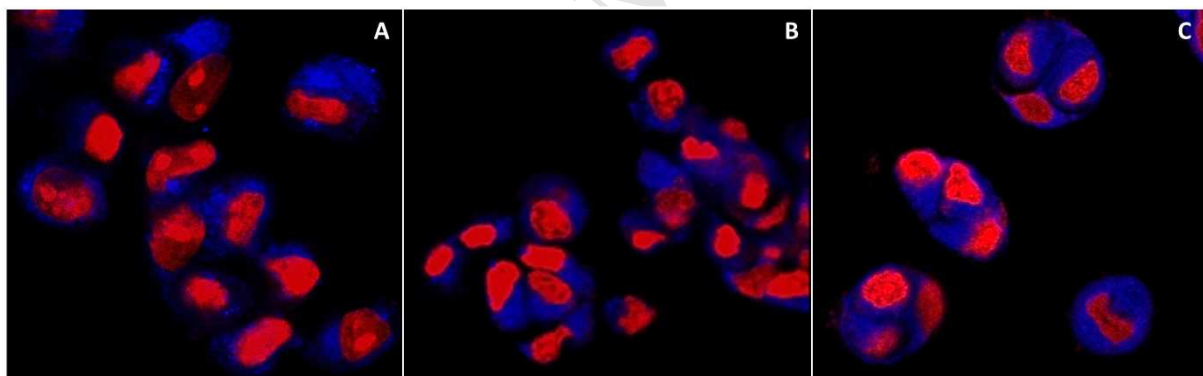


Figure 1. Subcellular localization of derivative **6e** in MCF7 cells. After 10 min (**A**) the compound (2 μ M, blue signal) distributes within the cytoplasm, the same localization was recorded after 30 min (**B**) and 1 h (**C**) post administration. Cellular nuclei were counterstained in red.

Thanks to its fluorescent properties, **6e** was detected using a confocal microscope (λ_{ex} 405 nm, λ_{em} 415-460 nm) (Figure S4). As depicted in Figure 1, **6e** rapidly entered MCF7 cells and widely

distributed into the whole cytoplasm, with some punctate accumulation visible within 10 min of exposure (Figure 1, panel A, 10 min, blue signal; Figure S3, panel 1). Thirty min - 1 h post administration (Figure 1, panels B and C; Figure S3, panels 2 and 3), **6e** subcellular localization remained in the cytoplasm: areas of more intense signal were still visible but randomly distributed, thus independent of intra-organelle accumulation, as reported for other photosensitizer. [43] No nuclear signal was ever detected.

Taken together, these results led us to investigate a cytosolic DNA-unrelated mechanism of cellular toxicity.

2.2.4 Spectroscopic and kinetic characterization of the triplet excited state of **6e**

To clarify the origin of the photocytotoxicity, we decided to provide a full characterization of the newly synthesized naphthyridine derivative **6e** as singlet oxygen sensitizer. Therefore, we preliminarily detected its lowest triplet-excited state (T_1) defining spectroscopic and kinetic features. In fact, it is well known that the population of a triplet excited state and its lifetime are both directly correlated to the efficiency of the generation of singlet oxygen. We set out to compare these issues for **6e**, the most photocytotoxic naphthyridine, with **5h**, the least photocytotoxic one. For solubility reasons, it was not possible to compare the two naphthyridines in aqueous media. Consequently, **6e** and **5h** were irradiated in acetonitrile by nanosecond laser flash photolysis (LFP), using a Nd:YAG laser, operating at 355 nm. Upon laser excitation at 355 nm, we recorded the transient absorption spectra in the range of 350-700 nm for both **6e** and **5h** (Figure 2a and 2b, respectively).

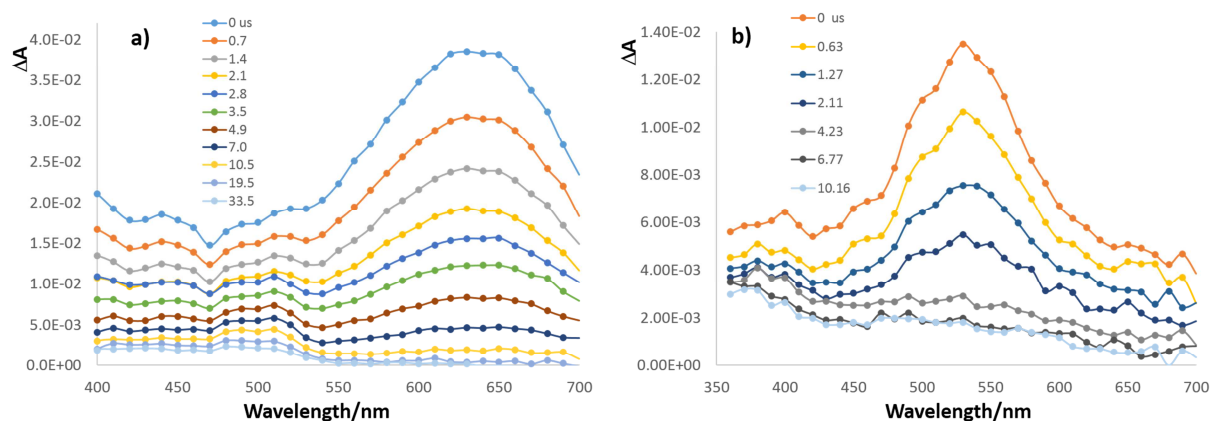


Figure 2. Time-resolved difference absorption spectra (ΔA) flashing argon-purged acetonitrile solutions of **6e** (1×10^{-4} M) (a) and **5h** (5×10^{-4} M) (b), at 355 nm.

A maximum of absorbance was recorded for both naphthyridine **6e** (λ_{\max} 650, Figure 2a) and **5h** (λ_{\max} 530 nm, Figure 2b). The transient absorption profiles decayed monoexponentially in air-equilibrated solutions with an identical lifetime of $\tau = 0.2 \mu\text{s}$. In argon-saturated solutions, the lifetime of the transient specie from **6e** became bi-exponential ($\tau_1 = 4.7 \mu\text{s}$, 18%; $\tau_2 = 18 \mu\text{s}$, 82%, Figure 3). Such an oxygen-dependent lifetime indicates that at the LFP pulse end we are very likely observing the triplet-state absorption of **6e**. A similar behaviour was also recorded for **5h**. The intensity of the signal assigned to the triplet excited states (T_1) of **6e** monitored at 650 nm ($A = 4.3 \times 10^{-2}$) was approximately 3 times more intense than that assigned to the T_1 of **5h** recorded at 530 nm ($A = 1.4 \times 10^{-2}$). Assuming that the molar extinction coefficients of T_1 are similar, all the data collected suggest that **5h** does not efficiently generate a triplet-excited state. Conversely, **6e** exhibiting T_1 with an exceptionally long 18.0 μs lifetime and a high molar absorptivity ($29781 \pm 180 \text{ M}^{-1}\text{cm}^{-1}$ at λ_{\max} 315 nm) may act as an interesting singlet oxygen sensitizer for biological applications.

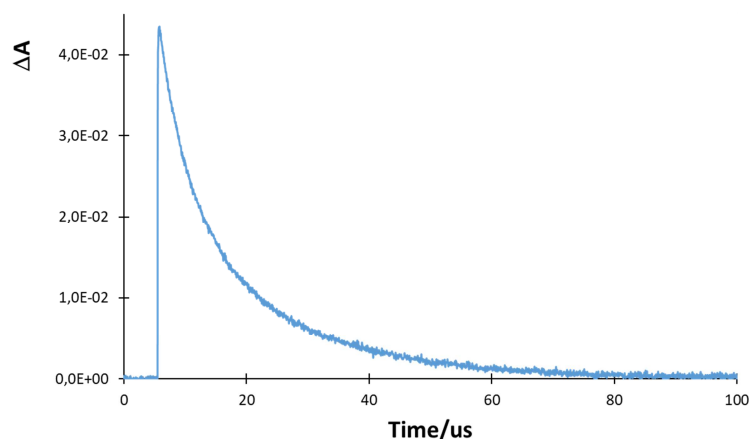


Figure 3. Triplet decay trace of **6e** monitored at 630 nm in neat acetonitrile under argon saturated condition.

2.2.5 Generation and trapping of $^1\text{O}_2$ by 9,10-anthracenedipropionic acid in aqueous acetonitrile

To further evaluate the efficiency of **6e** and **5h** as $^1\text{O}_2$ photosensitizer, we investigated the photo-oxidation of 9,10-anthracenedipropionic acid (ADPA), a water-soluble and efficient $^1\text{O}_2$ trap, forming a colourless endoperoxide via a [4 + 2] Diels-Alder cycloaddition. The photo-oxidation of ADPA by $^1\text{O}_2$ was followed monitoring the absorption at 400 nm, which indicates the consumption of the ADPA anthracene chromophore. [44] The experiments were carried out in aqueous acetonitrile (acetonitrile: water = 3:2). We did not use higher water content to avoid solubility issues for both **6e** and **5h**. The continuous photo-bleaching of the anthracene absorption in the presence of both **6e** and **5h**, monitored for 1 h at 315 nm excitation wavelength, indicated the photogeneration of $^1\text{O}_2$ (Figures S5 and S6). By-product formation was not detected during irradiation both by UV absorption and HPLC analysis. We did not record any decrease in the anthracene absorbance in the solutions without the sensitizer. We measured by ferrioxalate actinometry the efficiency of the ADPA consumption ($\Phi_{\text{R-315}}$: quantum yield) irradiating at 315

nm both naphthyridines. Surprisingly, the quantum yields for **6e** and **5h** were fairly low and very similar with $\Phi_{R-315} = 0.020 \pm 0.002$. The quantum yield for ADPA consumption using **6e** as 1O_2 sensitizer measured irradiating at 360 nm (Φ_{R-360}) was slightly higher ($\Phi_{R-360} = 0.025 \pm 0.003$). Buffering conditions in the same solvent did not substantially affect the quantum yield. We were not able to reliably measure Φ_{R-360} of **5h** irradiated at 360 nm, as its absorbance was negligible at that wavelength (Figure 4).

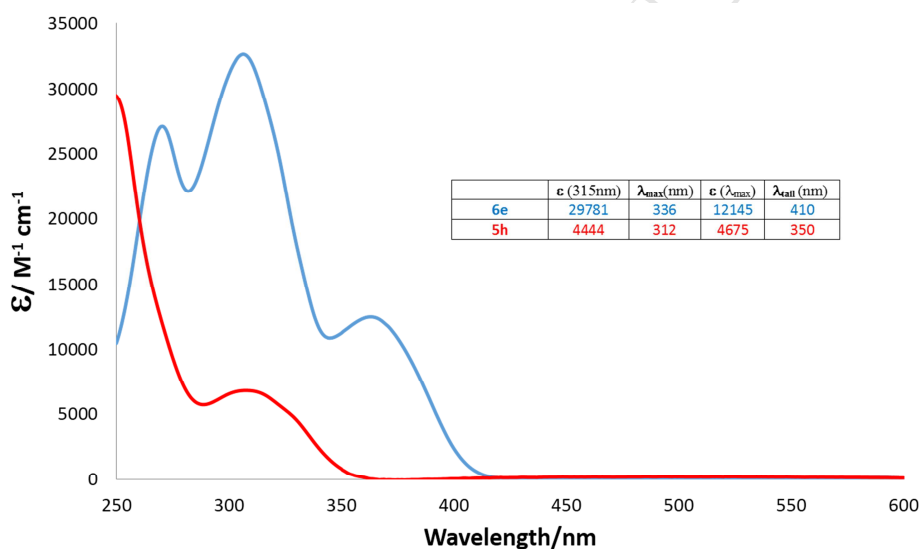


Figure 4. Absorbance comparison of **6e** (10^{-4} M) and **5h** (10^{-4} M) in acetonitrile: water = 3:2 solutions.

These data suggest that both **6e** and **5h** are capable to act as 1O_2 photosensitizers with comparable efficiency at 315 nm. The different photocytotoxicity described above, has to be ascribed to their differential optical properties, as **6e** exhibits much higher absorptivity at longer wavelength (with a tail above 400 nm) than **5h** (Figure 4).

2.2.5 Production of reactive oxygen species (ROS) upon UV irradiation

Generation of Reactive Oxygen Species (ROS) in cancer cells was next evaluated for compounds **6e** and **5h**. We employed the cell-permeant dichlorofluorescein (DCF) probe, which is converted to a highly fluorescent dye by ROS. Fluorescence in the presence/absence of UV irradiation ($\lambda \sim 365$ nm) was quantitatively evaluated in cells treated with the selected compounds; non-treated cells were used as negative controls. Cells treated with phorbol-12-myristate-13-acetate (PMA) and light activated were used as a positive control of intracellular ROS generation. [45,46] After 2 h from photoactivation, increasing concentrations of **6e** (0.5-2 μ M) showed a steady increase in fluorescence, which reached 227% of the untreated control (100%) at the highest concentration (Figure 5).

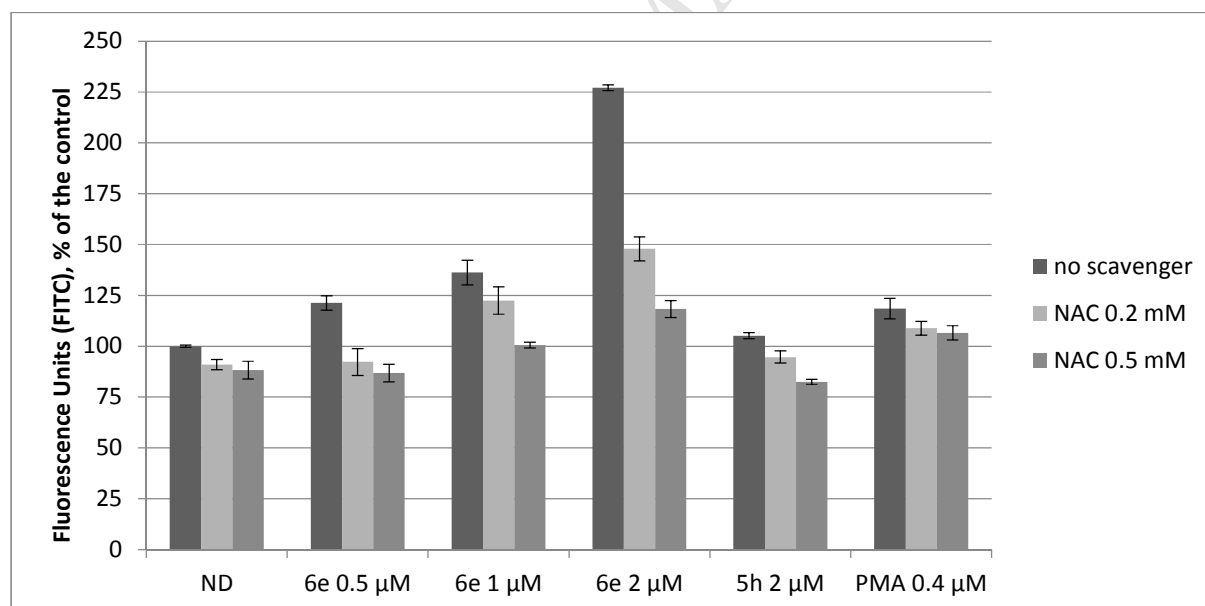


Figure 5. ROS production upon photoactivation of **6e** and **5h**. The increase in intracellular ROS levels was determined by a DCF-probe and was calculated as fluorescence increase compared to untreated irradiated controls. Assays were performed on non-treated (control), **6e**, **5h** and PMA treated cells, after 2 h from light exposure, in minimal medium (no scavenger) and in medium

containing an antioxidant compound at various concentration (i.e. N-acetylcysteine, NAC 200 nM and 500 nM). Results from three independent experiments are shown.

Conversely, treatment with **5h** or the administration of compounds without UV exposure did not modify control levels of fluorescence (Figure S7). The positive control sample (PMA, 400 nM) reached 120% of the untreated control 2 h after photoactivation (Figure 5). These data indicate that generation of ROS in cells by **6e** is massive and rises more rapidly than that mediated by the ROS inductor PMA. Moreover, compared to other ROS-inducer photosensitizers previously published by us, [17,18] **6e** resulted more potent and active at much lower concentration. To support the relevance of **6e**-induced ROS, we pre-incubated cells with the ROS scavenger N-acetylcysteine (NAC, 200-500 nM) and observed that NAC significantly reduced the generation of reactive species, in a dose dependent manner (Figure 5). [47] These results indicate that **6e** promptly and massively produces ROS in cells. Statistical analysis (Two tailed Student's t-test, P-value < 0.01) indicated that ROS levels measured in **6e**-treated cells were significant, while **5h**-treated cells were not significantly different from control samples. NAC-induced ROS depletion was significant in all samples.

2.2.6 Cytotoxicity mechanisms: cell death pathways

As production of copious amounts of ROS can trigger cell death by several different pathways, we next examined which mechanism (apoptosis or necrosis) of cell death was induced by **6e**.

The first feature that was taken into consideration was the distribution of MCF-7 cells in the cell cycle phases 24 h after administration of compounds **6e** and **5h**. The exposure of MCF7 cells to **6e** upon UV-activation did not alter the distribution of the cells in the different phases of the cell cycle (Figure S8), as assessed by flow cytometry analysis (PI staining, living cell population).

Statistical analysis also confirmed that cell population distribution in treated cells was not significantly altered in treated samples. This result suggested that cell death that could be related to a rapid and harsh intracellular damage rather than block during the normal cell cycle. To shed light on this aspect, a double staining (PI and Annexin V FITC) flow cytometry analysis was performed to discriminate the early and late stages of apoptosis. The presence of necrosis was also evaluated. MCF7 cells were treated with **6e** and **5h** at increasing concentrations (EC_{25} , EC_{50} and EC_{75} or EC_{50} respectively) and the whole cell population was analyzed. [48] At 4 h post photoactivation, 44-60% (depending on the drug concentration) of cells treated with compound **6e** showed features of non-living cells and were classified as apoptotic (34-50%), or necrotic (10%) cells (Figure 6).

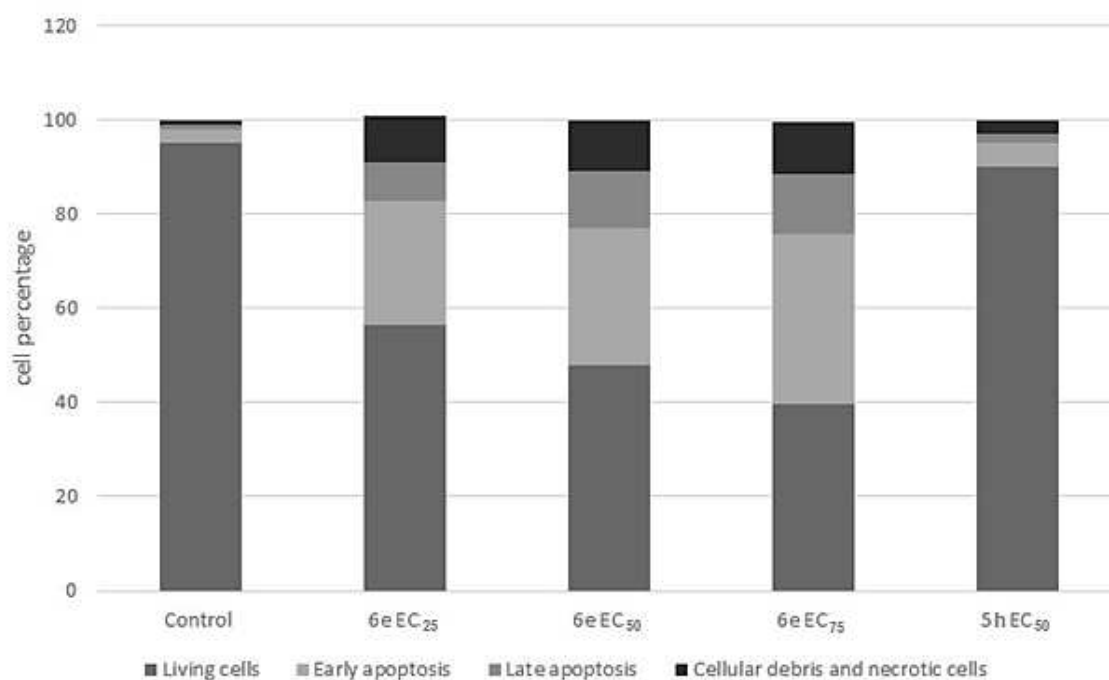


Figure 6. Cell population analysis. MCF7 cells were treated with **6e** at various concentrations (EC_{25} , EC_{50} and EC_{75}) and **5h** at EC_{50} and double stained with 7AAD and PE Annexin V 4 h after photoirradiation. Reported values represent the mean of three independent experiments.

In contrast, control cells and cells treated with **5h** were characterized by a large fraction of living cells (95% and 90%, respectively) and displayed only low amounts of apoptotic and necrotic cells (4% and 7%, respectively). These results evidenced that the administration and subsequent photoactivation of active compound **6e** caused a massive and very rapid cell death in tumor cells. Student T-test (two tailed, $P < 0.01$) was performed and assessed that data obtained for **6e**-treated cells were statistically significant, while **5h**-treated cells were comparable to control non-treated cells. As compared to other photoactivated compounds, oxazolo-derivatives pushed the majority of cell population into an irreversible apoptotic process in a shorter time lapse. [17,18] The triggering of apoptosis is a favourable feature for a chemotherapeutic drug, since, unlike necrosis, the apoptotic process does not cause an inflammatory reaction.

2.2.7 Cytotoxicity mechanisms: mitochondrial and lysosomal-dependent ROS response

Different intracellular signaling pathways, including mitochondrial dysfunction and lysosome activation, trigger and carry on the apoptotic process; we thus proceeded examining both mitochondrial and lysosomal involvement in **6e**-treated photoactivated cells. The induction of mitochondrial dysfunction was assessed with a mitochondrial membrane fluorescent probe, which allows to monitor morphology and mitochondria distribution within the cells. Untreated and treated cells with/without UV irradiation, were evaluated by confocal imaging. Control cells (untreated and non-irradiated) displayed the typical pattern of mitochondrial organization

reported for the MCF7 cell line, characterized by a more fragmented network compared to non-metastatic breast cancer cells (Figure 7, panel A). [49-51]

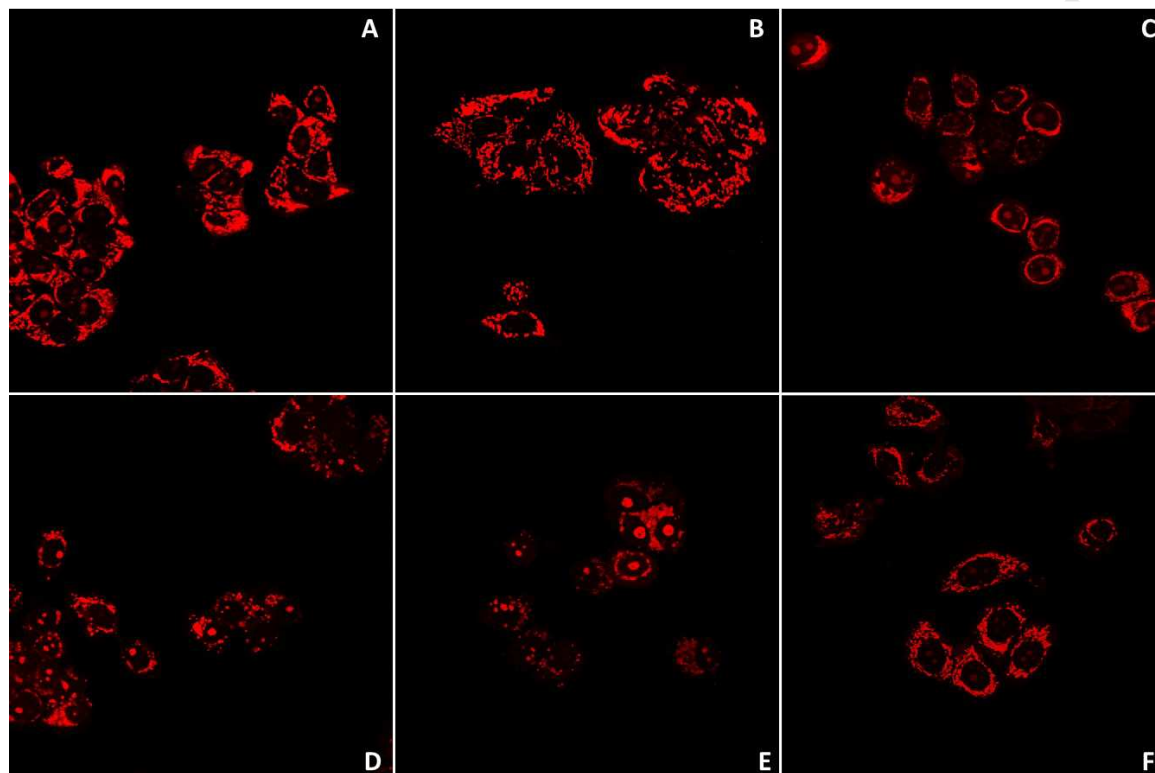


Figure 7. Mitochondrial morphology modifications induced by light-activated **6e** and **5h**. Mitochondrial membranes were visualized with a membrane potential-specific red fluorescent probe. **A**: non-treated and non-irradiated cells; **B**: non-treated and irradiated cells and **C**: PMA-treated cells (400 nM). **D**: **6e**, 2 μ M, 20 min after UV exposure; **E**: **6e**, 2 μ M, 2 h after UV exposure; **F**: **5h**, 2 μ M, 2 h after UV exposure. Well-defined mitochondrial network morphology was stained in non-treated cells, irradiated and non-irradiated, as well as in **5h** treated and irradiated cells (**A**, **B** and **C**). Cells treated with **6e**, following photoactivation, underwent significant mitochondrial network impairment and organelles swelling, already visible after 20 min (**D** and **E**). PMA was used as ROS-inducer positive control: a condensed mitochondrial network was visible 6 h post treatment (**F**).

Cells irradiated in the absence of ROS-generating compounds as well as cells treated with the compounds and non-irradiated were characterized by a similar mitochondrial network (Figure 7 and Figure S9, panel B; Figure S10, panels B-C). Notably, UV-activated **6e** caused an early remodeling of mitochondrial network, characterized by perinuclear clustering (Figure 7 and S9, panel D), followed by organelles fusion and mild swelling (Figure 7 and S9, panel E). This effect burst soon after UV exposure (20 min) and was even more intense 2 h after compound photoactivation. Conversely, **5h** in the same conditions did not induce any detectable mitochondrial perturbation (Figure 7, panel F). Treatment with PMA induced moderate mitochondria fusion after 6 h of treatment (Figure 7, panel C).

To further characterize the UV-activated **6e** induced cell death, the lysosomal involvement in the apoptotic process was also evaluated. A fluorescent probe able to stain acidic subcellular compartments, such as lysosomes and endosomes, was used. Cells treated with **6e** that also underwent UV irradiation showed considerable lysosomes activation, visible as bright green dots within the cytoplasm. Lysosomes activation was detectable 20 min after compound activation (green signal, Figure 8, panels D-E).

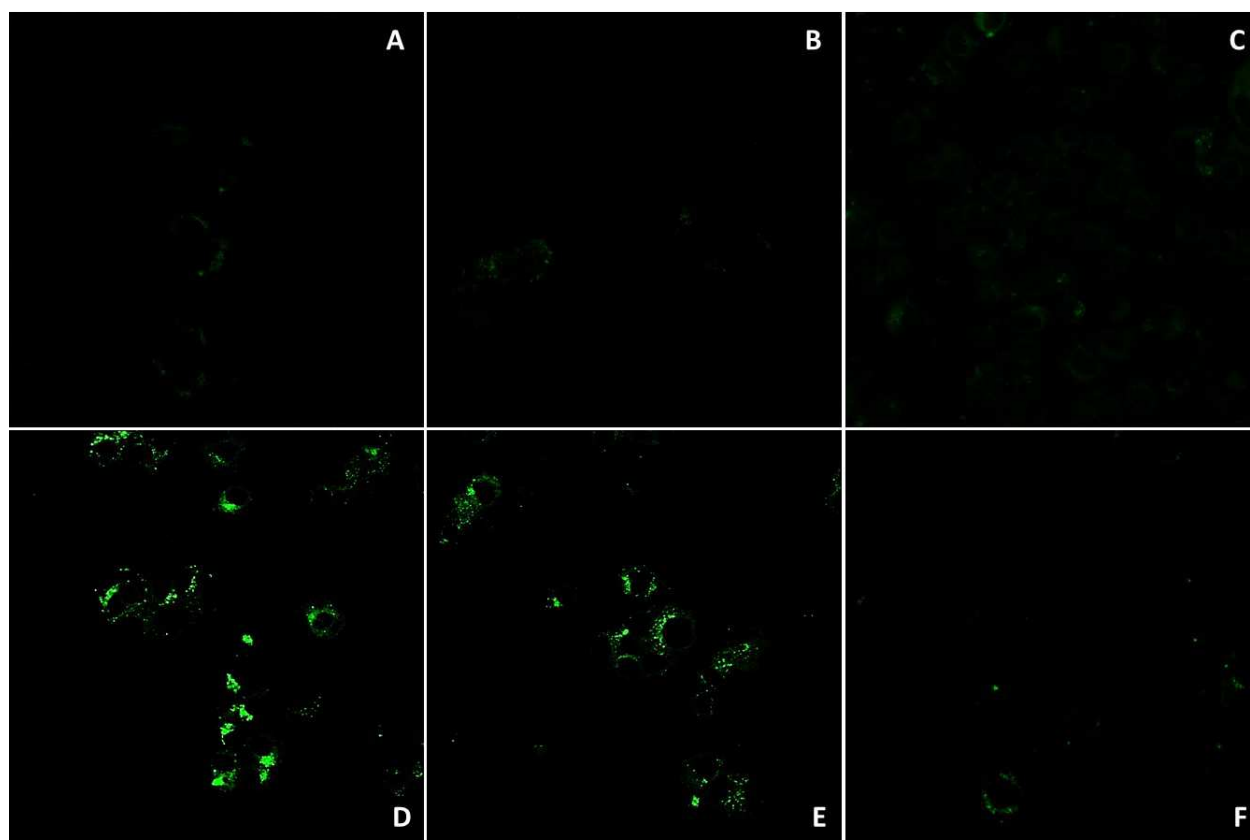


Figure 8. Lysosomes activation induced by UV-activated **6e** and **5h**. Lysosomes were visualized with a green fluorescent probe. **A**: non-treated and non-irradiated cells; **B**: non-treated and irradiated cells and **C**: PMA-treated cells (400 nM). **D**: **6e**, 2 μ M, 20 min after UV exposure; **E**: **6e**, 2 μ M, 2 h after UV exposure; **F**: **5h**, 2 μ M, 2 h after UV exposure. Non-treated MCF7 cells, irradiated and non-irradiated, showed none or minimal lysosome activation (**A** and **B**), as well as cells treated with **5h**. UV-activated **6e** displays a punctate distributed lysosomal activation after 20 min. After 2 h considerable lysosomal membrane depolarization was obtained, but lysosomes retain their shape and distribution within the cytoplasm.

The weak fluorescence detected in the cytoplasm indicated lysosomal membrane permeabilization, likely linked to the ROS outburst. [52,53] Two h after treatment, the probe signal decreased, although clear perinuclear punctate staining was still visible, indicating an

augmented lysosomal membrane permeabilization and an ongoing late apoptotic phase. [53] PMA treatment (400 nM, 6 h after treatment) induced a minimal lysosome signal (Figure 8, panel C). In contrast, cell treatment with **5h** in the presence/absence of UV irradiation did not induce lysosome activation (Figure 8, panel F; Figure S10, panel F). Similarly, non-treated control cells, with and without UV irradiation displayed negligible fluorescent signal (Figure 8, panels A-B; Figure S10, panels D-E).

Altogether, these studies demonstrated that ROS generation was necessary for naphthyridines-mediated cytotoxicity. The antiproliferative effect was triggered by a burst of ROS levels that promptly induced an unquenchable apoptotic process in tumor cells, featured by lysosomal involvement.

3. Conclusions

In our continuing efforts aimed at the study of heterocyclic scaffold as precursors of new potential photosensitizing agents with improved properties, [1,2,3]triazolo[4,5-*h*][1,6]naphthyridines **5**, [1,2,3]triazolo[4,5-*h*][1,6]naphthyridin-8-ones **7**, [1,3]oxazolo[5,4-*h*][1,6]naphthyridines **6**, and [1,3]oxazolo[5,4-*h*][1,6]naphthyridin-8-ones **8** were prepared in moderate to good yield (40-65%) through a multistep procedure, in order to investigate their photochemotherapeutic activities. Phototoxicity against three tumor cell lines (MCF7, A375 and HT-29) was assessed; upon irradiation, oxazolo-naphthyridines of type **6**, expressed growth inhibitory activity at nanomolar/low micromolar concentrations (EC_{50} 0.010–6.587 μ M). In particular, the most potent derivative **6e** was very active against MCF7 cell line, which is usually not very sensitive to drugs, and exhibited high selectivity (SI=72-86) and photocytotoxicity indexes (PTI >5000), in spite of its low singlet oxygen quantum yield (Φ_{Δ} 0.02 at 315 nm). Photocytotoxicity of oxazolo-naphthyridine **6e** is strictly connected to its optical properties as it

exhibited high molar absorptivity ($29781 \pm 180 \text{ M}^{-1}\text{cm}^{-1}$ at λ_{max} 315 nm) than the least reactive of the series, with a tail above 400 nm. Laser flash photolysis studies revealed that derivative **6e** efficiently generated a triplet-excited state with an exceptionally long 18.0 μs lifetime.

It has to be said that both absorption wavelength ($\lambda < 380 \text{ nm}$) and the molar extinction coefficient are quite low to compare favourably with other well-investigated singlet oxygen sensitizers.

Cellular mechanisms of phototoxicity indicated that derivative **6e** is distributed in the cytoplasm, thus exerting a cytosolic DNA-unrelated mechanism of cellular toxicity. Upon UV-activation, **6e** promptly and massively produced ROS in cells even more rapidly than the ROS inducer PMA. Thus the antiproliferative effect was triggered by a burst of ROS levels that immediately induced an unquenchable apoptotic process selectively in tumor cells, with both lysosomal and mitochondrial involvement. These findings are of great relevance since indicate that **6e** may act as a very promising singlet oxygen sensitizer for biological applications, paving the way to further drug development.

4. Experimental

4.1 Chemistry

All melting points were taken on a Büchi melting point M-560 apparatus. IR spectra were determined in bromoform with a Shimadzu FT/IR 8400S spectrophotometer. ^1H and ^{13}C NMR spectra were measured at 200 and 50.0 MHz, respectively, in $\text{DMSO}-d_6$ or CDCl_3 solution, using a Bruker Avance II series 200 MHz spectrometer. Column chromatography was performed with Merk silica gel 230-400 mesh ASTM or with Büchi Sepacor chromatography module (prepacked cartridge system). Elemental analyses (C, H, N) were within $\pm 0.4\%$ of theoretical values and

were performed with a VARIO EL III elemental analyzer. The purity of all the tested compounds was >95%, determined by HPLC (Agilent 1100 series). In particular, (NH₄)₂HPO₄ 0.4 M/acetonitrile 68:32 v/v was used as eluent, with a flow rate of 1 mL/min, filtered on a cellulose regenerated filter, cut off 0.2 μm, and samples injected in a C18 Gemini HPLC column. The purity was calculated by using a calibration curve obtained for serially diluted concentrations of compounds (K_{max} = 254 nm) in the eluent and expressed as the amount of intact molecules per unit mass.

General procedures, analytical and spectroscopic data for compounds **13a-c**, were previously reported. [54,55]

Analytical and spectroscopic data for naphthyridine derivatives **5b**, **5e**, **5k**, **5l**, **6a**, **6c**, **6f**, **6g**, **6k** and naphthyridine-8-ones **7c**, **8b** and **8c** were reported in the supporting information.

4.1.1 General Procedure for the Synthesis of 5-Amino-1-substituted-1*H*-1,2,3-triazole-4-carbonitrile derivatives (17a-c)

To a solution of sodium ethoxide (0.29 g, 4.30 mmol) in anhydrous ethanol (10 mL), malononitrile **14** (0.27 g, 4.08 mmol) was added and the reaction was stirred at room temperature for 15 min. Then the solution of the suitable azido derivative **13a-c** (3.40 mmol) in anhydrous ethanol (10 mL) was added at 0 °C and the reaction mixture was stirred at room temperature for 12 h. The solvent was removed under reduced pressure and the crude product was purified by chromatography (DCM/AcOEt 95/5)

4.1.1.1 5-Amino-1-phenyl-1*H*-1,2,3-triazole-4-carbonitrile (17a)

Light brown; yield: 60%; mp: 125.5-126.6 °C; IR cm⁻¹: 3380, 3330 (NH₂), 2249 (CN); ¹H NMR (200 MHz, CDCl₃) δ: 5.02 (2H, bs, NH₂), 7.50-7.63 (5H, m, Ar); ¹³C NMR (50 MHz, CDCl₃) δ:

103.9 (s), 112.4 (s), 124.4 (2 x d), 130.4 (d), 130.5 (2 x d), 136.7 (s), 146.6 (s). Anal. Calcd for C₉H₇N₅: C, 58.37; H, 3.81; N, 37.82. Found: C, 58.15; H, 3.92; N, 37.74.

4.1.1.2 5-Amino-1-(4-methoxyphenyl)-1*H*-1,2,3-triazole-4-carbonitrile (17b)

Light brown; yield: 70%; mp: 189.5-190.0 °C; IR cm⁻¹: 3347, 3290 (NH₂), 2234 (CN); ¹H NMR (200 MHz, DMSO-*d*₆) δ: 3.84 (3H, s, CH₃O), 7.02 (2H, bs, NH₂), 7.14 (2H, d, *J* = 10.0 Hz, H₂ and H₆), 7.23 (2H, d, *J* = 10.0 Hz, H₃ and H₅); ¹³C NMR (50 MHz, DMSO-*d*₆) δ: 55.6 (q), 100.9 (s), 113.5 (s), 114.9 (2 x d), 126.6 (s), 126.8 (2 x d), 148.0 (s), 160.0 (s). Anal. Calcd for C₁₀H₉N₅O: C, 55.81; H, 4.22; N, 32.54. Found: C, 55.93; H, 4.13; N, 32.45.

4.1.1.3 5-Amino-1-(3,4,5-trimethoxyphenyl)-1*H*-1,2,3-triazole-4-carbonitrile (17c)

Light brown; yield: 60%; mp: 173.3-174.0 °C; IR cm⁻¹: 3405, 3353 (NH₂), 2223 (CN); ¹H NMR (200 MHz, CDCl₃) δ: 3.90 (9H, s, 3 x CH₃O), 4.94 (2H, bs, NH₂), 6.70 (2H, s, H₂ and H₆); ¹³C NMR (50 MHz, CDCl₃) δ: 56.5 (2 x q), 61.1 (q), 100.0 (s), 102.1 (2 x d), 112.3 (s), 128.9 (s), 139.3 (s), 146.6 (s), 154.3 (2 x s). Anal. Calcd for C₁₂H₁₃N₅O₃: C, 52.36; H, 4.76; N, 25.44. Found: C, 52.48; H, 4.53; N, 25.35.

4.1.2 General Procedure for the Synthesis of 5-Amino-2-substituted[1,3]oxazole-4-carbonitrile derivatives (18a-c)

These compounds were synthesized according to the previously described procedure. [38] To a stirred solution of 1.7 g of aminomalononitrile tosylate **16** (4.6 mmol) in 1-methyl-2-pyrrolidinone (12 mL, 117.0 mmol) the suitable benzoyl chloride **15a-c** (5.1 mmol) was added. The reaction mixture was stirred at room temperature for 12 hours and then, diluted with 100 mL

of a 1:1 solution of ethyl acetate: ethyl ether, washed with water (2x100 mL), and a 10% saturated solution of sodium hydrogen carbonate (2x100 mL). The organic layer was dried over sodium sulphate and the solvent removed under reduced pressure.

4.1.2.1 5-Amino-2-phenyl[1,3]oxazole-4-carbonitrile derivatives (18a)

This compound was obtained in 79% yield. Analytical and spectroscopic data are in accordance to those reported in literature. [56]

4.1.2.2 5-Amino-2-(4-methoxyphenyl)[1,3]oxazole-4-carbonitrile (18b)

This compound was obtained in 51% yield. Analytical and spectroscopic data are in accordance to those reported in literature. [57]

4.1.2.3 5-Amino-2-(3,4,5-trimethoxyphenyl)-[1,3]oxazole-4-carbonitrile (18c)

White solid; yield: 58%; mp: 241.3-242.6 °C; IR cm^{-1} : 3328, 3216 (NH_2), 2221 (CN); ^1H NMR (200 MHz, $\text{DMSO-}d_6$) δ : 3.71 (3H, s, CH_3O), 3.84 (6H, s, $\text{CH}_3\text{O} \times 2$), 7.02 (2H, s, H_2' and H_6'), 8.01 (2H, s, NH_2); ^{13}C NMR (50 MHz, $\text{DMSO-}d_6$) δ : 55.8 (2 x q), 60.1 (q), 84.0 (s), 102.1 (2 x d), 115.3 (s), 121.3 (s), 138.9 (s), 149.2 (s), 153.2 (2 x s), 162.2 (s). Anal. Calcd. for $\text{C}_{13}\text{H}_{13}\text{N}_3\text{O}_4$: C, 56.72; H, 4.76; N, 15.27. Found: C, 56.53; H, 4.60; N, 15.45.

4.1.3 General Procedure for the Synthesis of Ethyl 7-amino-5-methyl-3-substituted-3H-[1,2,3]triazolo[4,5-b]pyridine-6-carboxylate derivatives (19a-c) and Ethyl 7-amino-5-methyl-2-substituted[1,3]oxazolo[5,4-b]pyridine-6-carboxylate derivatives (20a-c)

These compounds were synthesized according to the procedure reported in [56], slightly modified by us. To a mixture of ethyl acetoacetate (0.20 mL, 1.54 mmol) and 5-amino-1-substituted-1H-1,2,3-triazole-4-carbonitriles **17a-c** (1.27 mmol) or 5-amino-2-substituted[1,3]oxazole-4-carbonitriles **18a-c** (1.27 mmol) in anhydrous toluene (50 mL), stannic

chloride (0.18 mL, 1.54 mmol) was slowly added at 0°C. The mixture was refluxed for 2 hours using a Dean-Stark trap. After cooling 0.07 mmol of stannic chloride were added and the reaction mixture was further refluxed for 2 hours. After the complete depletion of the starting material, sodium hydroxide 5M solution was added to pH 10; the reaction mixture was extracted with AcOEt (3x50 mL). The organic layer was dried over sodium sulphate and the solvent removed under reduced pressure. The crude product was purified by chromatography (DCM/AcOEt 9/1).

4.1.3.1 Ethyl 7-amino-5-methyl-3-phenyl-3*H*-[1,2,3]triazolo[4,5-*b*]pyridine-6-carboxylate (19a)

White solid; yield: 45%; mp: 164.8 - 165.1 °C; IR cm^{-1} : 3496, 3359 (NH_2), 1680 (CO); ^1H NMR (200 MHz, CDCl_3) δ : 1.44 (3H, t, $J = 8.0$ Hz, CH_3), 2.84 (3H, s, CH_3), 4.43 (2H, q, $J = 8.0$ Hz, CH_2), 7.32 (2H, s, NH_2), 7.43 (1H, t, $J = 7.2$ Hz, H_4), 7.57 (t, 2H, $J = 7.2$ Hz, H_3 and H_5), 8.28 (d, 2H, $J = 7.2$ Hz, H_2 and H_6); ^{13}C NMR (50 MHz, CDCl_3) δ : 14.3 (q), 28.5 (q), 61.1 (t), 102.8 (s), 121.4 (2 x d), 128.0 (s), 128.1 (d), 129.4 (2 x d), 136.6 (s), 145.2 (s), 149.5 (s), 164.3 (s), 168.6 (s). Anal. Calcd for $\text{C}_{15}\text{H}_{15}\text{N}_5\text{O}_2$: C, 60.60; H, 5.09; N, 23.56. Found: C, 60.71; H, 4.89; N, 23.42.

4.1.3.2 Ethyl 7-amino-3-(4-methoxyphenyl)-5-methyl-3*H*-[1,2,3]triazolo[4,5-*b*]pyridine-6-carboxylate (19b)

White solid; yield: 62%; mp: 179.1-180.0 °C; IR cm^{-1} : 3448, 3333 (NH_2), 1688 (CO); ^1H NMR (200 MHz, CDCl_3) δ : 1.44 (3H, t, $J=8.0$ Hz, CH_3), 2.83 (3H, s, CH_3), 3.88 (3H, s, CH_3O), 4.46 (2H, q, $J = 8.0$ Hz, CH_2), 7.08 (2H, d, $J = 8.0$ Hz, H_2 and H_6), 7.28 (2H, bs, NH_2), 8.12 (2H, d, $J = 8.0$ Hz, H_3 and H_5); ^{13}C NMR (50 MHz, CDCl_3) δ : 14.3 (q), 28.5 (q), 55.6 (q), 61.0 (t), 102.7 (s), 114.6 (2 x d), 123.2 (2 x d), 127.8 (s), 129.7 (s), 145.0 (s), 149.4 (s), 159.3 (s), 164.2 (s),

168.7 (s). Anal. Calcd for C₁₆H₁₇N₅O₃: C, 58.71; H, 5.23; N, 21.39. Found: C, 58.54; H, 5.30; N, 21.48.

4.1.3.3 Ethyl 7-amino-5-methyl-3-(3,4,5-trimethoxyphenyl)-3H-[1,2,3]triazolo[4,5-*b*]pyridine-6-carboxylate (19c)

White solid; yield: 50%; mp: 192.9-193.7 °C; IR cm⁻¹: 3455, 3398 (NH₂), 1680 (CO); ¹H NMR (200 MHz, DMSO-*d*₆) δ: 1.34 (3H, t, *J* = 8.2 Hz, CH₃), 2.66 (3H, s, CH₃), 3.74 (3H, s, CH₃O), 3.88 (6H, s, CH₃O_{x2}), 4.35 (2H, q, *J* = 8.2 Hz, CH₂), 7.56 (2H, s, H₂ and H₆), 8.06 (2H, s, NH₂); ¹³C NMR (50 MHz, DMSO-*d*₆) δ: 14.0 (q), 27.1 (q), 56.1 (2 x q), 60.2 (q), 61.0 (t), 99.2 (2 x d), 99.5 (s), 99.6 (s), 103.4 (s), 131.8 (s), 114.9 (s), 148.1 (s), 153.2 (2 x s), 162.2 (s), 167.4 (s). Anal. Calcd for C₁₈H₂₁N₅O₅: C, 55.81; H, 5.46; N, 18.08. Found: C, 55.94; H, 5.32; N, 17.94.

4.1.3.4 Ethyl 7-amino-5-methyl-2-phenyl[1,3]oxazolo[5,4-*b*]pyridine-6-carboxylate (20a)

This compound was obtained in 45% yield. Analytical and spectroscopic data are in accordance to those reported in literature. [58]

4.1.3.5 Ethyl 7-amino-2-(4-methoxyphenyl)-5-methyl[1,3]oxazolo[5,4-*b*]pyridine-6-carboxylate (20b)

White solid; yield: 65%; mp: 173.2-173.5 °C; IR cm⁻¹: 3415, 3321 (NH₂), 1670 (CO); ¹H NMR (200 MHz, CDCl₃) δ: 1.44 (3H, t, *J* = 7.2 Hz, CH₃), 2.79 (3H, s, CH₃), 3.89 (3H, s, CH₃O), 4.42 (2H, q, *J* = 7.2 Hz, CH₂), 6.61 (2H, s, NH₂), 7.01 (2H, d, *J* = 8.6 Hz, H₃ and H₅), 8.12 (2H, d, *J* = 8.6 Hz, H₂ and H₆); ¹³C NMR (50 MHz, CDCl₃) δ: 14.3 (q), 27.4 (q), 55.4 (q), 61.0 (t), 105.9 (s), 114.4 (2 x d), 119.3 (s), 119.4 (s), 128.9 (2 x d), 148.6 (s), 158.6 (s), 159.4 (s), 159.9 (s), 162.2 (s), 168.6 (s). Anal. Calcd. for C₁₇H₁₇N₃O₄: C, 62.38; H, 5.23; N, 12.84. Found: C, 62.20; H, 5.15; N, 12.97.

4.1.3.6 Ethyl 7-amino-5-methyl-2-(3,4,5-trimethoxyphenyl)[1,3]oxazolo[5,4-*b*]pyridine-6-carboxylate (**20c**)

White solid; yield: 45%; mp: 183.4-185 °C; IR cm^{-1} : 3450, 3350 (NH_2), 1674 (CO); ^1H NMR (200 MHz, $\text{DMSO-}d_6$) δ : 1.45 (3H, t, $J = 7.2$ Hz, CH_3), 2.79 (3H, s, CH_3), 3.93 (3H, s, CH_3O), 3.97 (6H, s, 2 x CH_3O), 4.43 (2H, q, $J = 7.2$ Hz, CH_2), 6.66 (2H, s, NH_2), 7.44 (2H, s, H_2 and H_6); ^{13}C NMR (50 MHz, $\text{DMSO-}d_6$) δ : 14.3 (q), 27.5 (q), 56.3 (2 x q), 61.0 (q), 61.1 (t), 104.2 (2 x d), 106.0 (s), 119.2 (s), 121.9 (s), 140.9 (s), 148.9 (s), 153.6 (2 x s), 159.1 (s), 159.4 (s), 159.5 (s), 168.6 (s). Anal. Calcd. for $\text{C}_{19}\text{H}_{21}\text{N}_3\text{O}_6$: C, 58.91; H, 5.46; N, 10.85. Found: C, 58.80; H, 5.32; N, 11.01.

4.1.4 General Procedure for the Synthesis of (7-amino-5-methyl-3-substituted-3*H*-[1,2,3]triazolo[4,5-*b*]pyridin-6-yl)methanol derivatives (**21a-c**) and (7-amino-5-methyl-2-substituted[1,3]oxazolo[5,4-*b*]pyridin-6-yl)methanol derivatives (**22a-c**)

To a suspension of lithium aluminium hydride (0.07 g, 2.11 mmol) in anhydrous tetrahydrofuran (10 mL), the suitable ethyl 7-amino-5-methyl-3-substituted-3*H*-[1,2,3]triazolo[4,5-*b*]pyridine-6-carboxylate **19a-c** (0.64 mmol) or ethyl 7-amino-5-methyl-2-substituted-[1,3]oxazolo[5,4-*b*]pyridine-6-carboxylate **20a-c** (0.64 mmol) was added at 0° C and the resulting suspension was stirred at room temperature for 12 h. The reaction mixture was poured onto crushed ice. The precipitate was filtered, dried and washed with diethyl ether.

4.1.4.1 (7-Amino-5-methyl-3-phenyl-3*H*-[1,2,3]triazolo[4,5-*b*]pyridin-6-yl)methanol (**21a**)

White solid; yield: 92%; mp: >350°C; IR cm^{-1} : 3460 (OH), 3421, 3335 (NH_2); ^1H NMR (200 MHz, $\text{DMSO-}d_6$) δ : 2.58 (3H, s, CH_3), 4.61 (2H, d, $J = 5.2$ Hz, CH_2), 4.84 (1H, t, $J = 5.2$ Hz, OH), 7.12 (2H, s, NH_2), 7.48 (1H, t, $J = 7.3$ Hz, H_4), 7.65 (2H, t, $J = 7.3$ Hz, H_3 and H_5), 8.26

(2H, d, $J = 7.3$ Hz, $H_{2'}$ and $H_{6'}$); ^{13}C NMR (50 MHz, $\text{DMSO-}d_6$) δ : 23.4 (q) \square 55.5 (t), 111.8 (s), 120.8 (2 x d), 127.6 (s), 127.9 (2 x d), 129.5 (d), 136.6 (s), \square 144.6 (s), 145.8 (s), 160.1 (s). Anal. Calcd for $\text{C}_{13}\text{H}_{13}\text{N}_5\text{O}$: C, 61.17; H, 5.13; N, 27.43. Found: C, 61.23; H, 5.01; N, 27.54.

4.1.4.2 (7-amino-3-(4-methoxyphenyl)-5-methyl-3H-[1,2,3]triazolo[4,5-b]pyridin-6-yl)methanol (21b)

White solid; yield: 58%; mp: $>350^\circ\text{C}$; IR cm^{-1} : 3439 (OH), 3347, 3238 (NH_2); ^1H NMR (200 MHz, $\text{DMSO-}d_6$) δ : 2.56 (3H, s, CH_3), 3.85 (3H, s, CH_3O), 4.60 (2H, d, $J = 5.1$ Hz, CH_2), 4.82 (1H, t, $J=5.1$ Hz, OH), 7.07 (2H, s, NH_2), 7.19 (2H, d, $J = 7.1$ Hz, $H_{2'}$ and $H_{6'}$), 8.09 (2H, d, $J = 7.1$ Hz, $H_{3'}$ and $H_{5'}$); ^{13}C NMR (50 MHz, $\text{DMSO-}d_6$) δ : 23.4 (q) \square 55.4 (q), 55.5 (t), 111.6 (s), 114.5 (2 x d), 122.7 (2 x d), 127.8 (s), 129.6 (s), 144.4 (s), 145.7 (s), \square 158.5 (s), 159.9 (s). Anal. Calcd for $\text{C}_{14}\text{H}_{15}\text{N}_5\text{O}_2$: C, 58.94; H, 5.30; N, 24.55. Found: C, 58.83; H, 5.42; N, 24.63.

4.1.4.3 (7-amino-5-methyl-3-(3,4,5-trimethoxyphenyl)-3H-[1,2,3]triazolo[4,5-b]pyridin-6-yl)methanol (21c)

White solid; yield: 88%; mp: $>350^\circ\text{C}$; IR cm^{-1} : 3513 (OH), 3349, 3341 (NH_2); ^1H NMR (200 MHz, $\text{DMSO-}d_6$) δ : 2.58 (3H, s, CH_3), 3.74 (3H, s, CH_3O), 3.89 (6H, s, 2 x CH_3O), 4.60 (2H, d, $J = 4.8$ Hz, CH_2), 4.83 (1H, t, $J = 4.8$ Hz, OH), 7.13 (2H, s, NH_2) 7.66 (2H, s, $H_{2'}$ and $H_{6'}$); ^{13}C NMR (50 MHz, $\text{DMSO-}d_6$) δ : 23.6 (q), 55.4 (t), 56.0 (2 x q), 60.2 (q), 98.4 (2 x d), 111.8 (s), 128.0 (s), 132.5 (s), 136.5 (s), 144.5 (s), 145.8 (s), 159.2 (2 x s), 159.9 (s). Anal. Calcd for $\text{C}_{16}\text{H}_{19}\text{N}_5\text{O}_4$: C, 55.64; H, 5.55; N, 20.28. Found: C, 55.77; H, 5.43; N, 20.19.

4.1.4.4 (7-Amino-5-methyl-2-phenyl[1,3]oxazolo[5,4-b]pyridin-6-yl)methanol (22a)

White solid; yield: 80%; mp: $>350^\circ\text{C}$; IR cm^{-1} : 3460 (OH), 3421, 3335 (NH_2); ^1H NMR (200 MHz, $\text{DMSO-}d_6$) δ : 3.36 (3H, s, CH_3), 4.5 (2H, d, $J = 5.2$ Hz, CH_2), 4.87 (1H, t, $J = 5.2$ Hz,

OH), 6.52 (2H, s, NH₂), 7.59-7.62 (3H, m, ArH), 8.10-8.15 (2H, m, ArH); ¹³C NMR (50 MHz, DMSO-*d*₆) δ: 22.7 (q) 59.3 (t), 113.9 (s), 127.9 (s), 127.7 (2 x d), 127.3 (2 x d), 128.9 (d), 131.3 (s), 132.1 (s), 146.3 (s), 152.5 (s), 159.1 (s). Anal. Calcd. for C₁₄H₁₃N₃O₂: C, 65.87; H, 5.13; N, 16.46. Found: C, 65.68; H, 5.00; N, 16.60.

4.1.4.5 (7-amino-2-(4-methoxyphenyl)-5-methyl[1,3]oxazolo[5,4-*b*]pyridin-6-yl)methanol (22b)

White solid; yield: 55%; mp: >350 °C; IR cm⁻¹: 3498 (OH), 3410, 3339 (NH₂); ¹H NMR (200 MHz, DMSO-*d*₆) δ: 2.47 (3H, s, CH₃), 3.86 (3H, s, CH₃O), 4.5 (2H, d, *J* = 5.4 Hz, CH₂), 4.86 (1H, t, *J* = 5.4 Hz, OH), 6.44 (2H, s, NH₂), 7.16 (2H, d, *J* = 8.8 Hz, H_{3'} and H_{5'}), 8.08 (2H, d, *J* = 8.8 Hz, H_{2'} and H_{6'}); ¹³C NMR (50 MHz, DMSO-*d*₆) δ: 22.4 (q), 55.4 (q), 55.9 (t), 114.6 (s), 114.7 (2 x d), 118.3 (s), 119.2 (s), 128.3 (2 x d), 146.0 (s), 152.6 (s), 157.5 (s), 158.3 (s), 161.6 (s). Anal. Calcd. for C₁₅H₁₅N₃O₃: C, 63.15; H, 5.30; N, 14.73. Found: C, 63.04; H, 5.22; N, 14.81.

4.1.4.6 (7-amino-5-methyl-2-(3,4,5-trimethoxyphenyl)[1,3]oxazolo[5,4-*b*]pyridin-6-yl)methanol (22c)

White solid; yield: 78%; mp: >350 °C; IR cm⁻¹: 3496 (OH), 3421, 3335 (NH₂); ¹H NMR (200 MHz, DMSO-*d*₆) δ: 3.36 (3H, s, CH₃), 3.76 (3H, s, CH₃), 3.91 (6H, s, CH₃), 4.56 (2H, d, *J* = 4.6 Hz, CH₂), 4.87 (1H, t, *J* = 4.6 Hz, OH), 6.53 (2H, s, NH₂), 7.40 (2H, s, H_{2'} and H_{6'}); ¹³C NMR (50 MHz, DMSO-*d*₆) δ: 22.5 (q) 55.9 (t), 56.0 (2 x q), 60.2 (q), 103.6 (2 x d), 114.7 (s), 118.3 (s), 122.1 (s), 140.0 (s), 146.2 (s), 153.0 (s), 153.3 (2 x s), 157.2 (s), 158.4 (s). Anal. Calcd. for C₁₆H₁₉N₃O₅: C, 59.12; H, 5.55; N, 12.17;. Found: C, 59.27; H, 5.63; N, 12.02.

4.1.5 General Procedure for the Synthesis of 7-Amino-5-methyl-3-substituted-3*H*-[1,2,3]triazolo[4,5-*b*]pyridine-6-carbaldehyde derivatives (**23a-c**) and 7-Amino-5-methyl-2-substituted-[1,3]oxazolo[5,4-*b*]pyridine-6-carbaldehyde derivatives (**24a-c**)

To a solution of the suitable 7-amino-5-methyl-3-substituted-3*H*-[1,2,3]triazolo[4,5-*b*]pyridin-6-yl)methanol derivatives **21a-c** (1.74 mmol) or (7-amino-5-methyl-2-substituted-[1,3]oxazolo[5,4-*b*]pyridin-6-yl)methanol derivatives **22a-c** (1.74 mmol) in anhydrous dichloromethane (20 mL), Dess-Martin periodinane (1.03 g, 2.44 mmol) was gradually added under argon atmosphere. The reaction mixture was stirred at room temperature for 5 hours; diethyl ether was added and the organic phase was washed with a 5% solution of sodium thiosulfate and a saturated solution of sodium hydrogen carbonate. The organic phase was dried over sodium sulfate and the solvent was removed under reduced pressure to give the crude carbaldehyde derivative product which was immediately used in the next step.

4.1.6 General Procedure for the Synthesis of 5-Methyl-3,8-disubstituted-3*H*-[1,2,3]triazolo[4,5-*h*][1,6]naphthyridine derivatives (**5a-l**) and 5-Methyl-2,8-disubstituted[1,3]oxazolo[5,4-*h*][1,6]naphthyridine derivatives (**6a-l**)

To a solution of 7-amino-5-methyl-2-substituted-[1,3]triazolo[5,4-*b*]pyridine-6-carbaldehyde derivatives **23a-c** (0.30 mmol) or 7-amino-5-methyl-2-substituted[1,3]oxazolo[5,4-*b*]pyridine-6-carbaldehyde derivatives **24a-c** (0.30 mmol) and potassium hydroxide (0.02 g, 0.36 mmol) in ethanol or acetone (for derivatives **5d**, **5h**, **5l**, **6d**, **6h**, **6l**), the proper ketone (0.30 mmol) was added. The reaction mixture was heated under reflux for 12 h. Then the reaction mixture was poured onto crushed ice and the precipitate was filtered off, dried and purified by chromatography (DCM/AcOEt 95/5).

4.1.6.1 5-Methyl-3,8-diphenyl-3H-[1,2,3]triazolo[4,5-*h*][1,6]naphthyridine (5a)

This compound was obtained from reaction of **23a** with acetophenone. White solid; yield: 45%; mp: 262.8-263.0 °C; ¹H NMR (200 MHz, CDCl₃) δ: 3.06 (3H, s, CH₃), 7.48-7.65 (6H, m, ArH), 8.05 (1H, d, *J* = 8.8 Hz, H₇), 8.31-8.40 (4H, m, ArH), 8.54 (1H, d, *J* = 8.8 Hz, H₆); ¹³C NMR (50 MHz, CDCl₃) δ: 23.1 (q), 119.2 (d), 119.5 (s), 122.2 (2 x d), 128.2 (2 x d), 128.4 (d), 128.9 (2 x d), 129.5 (2 x d), 130.7 (d), 133.3 (s), 135.9 (d), 136.5 (s), 137.9 (s), 143.9 (s), 144.1 (s), 161.7 (s), 162.2 (s). Anal. Calcd for C₂₁H₁₅N₅: C, 74.76; H, 4.48; N, 20.76. Found: C, 74.83; H, 4.32; N, 20.65.

4.1.6.2 8-(4-Methoxyphenyl)-5-methyl-3-phenyl-3H-[1,2,3]triazolo[4,5-*h*][1,6]naphthyridine (5c)

This compound was obtained from reaction of **23a** with 4-methoxy-acetophenone. White solid; yield: 53%; mp: 227.8-228.0 °C; ¹H NMR (200 MHz, CDCl₃) δ: 3.04 (3H, s, CH₃), 3.91 (3H, s, CH₃O), 7.06 (2H, d, *J* = 6.9 Hz, ArH), 7.45-7.66 (3H, m, ArH), 7.98 (1H, d, *J* = 8.9 Hz, H₇), 7.32-8.38 (4H, m, ArH), 8.48 (1H, d, *J* = 8.9 Hz, H₆); ¹³C NMR (50 MHz, CDCl₃) δ: 23.0 (q), 55.5 (q), 114.3 (2 x d), 118.5 (d), 119.1 (s), 122.2 (2 x d), 128.4 (d), 129.4 (2 x d), 129.8 (2 x d), 130.4 (s), 133.4 (s), 135.6 (d), 136.6 (s), 144.0 (s), 144.2 (s), 161.2 (s), 161.9 (s), 162.1 (s). Anal. Calcd for C₂₂H₁₇N₅O: C, 71.92; H, 4.66; N, 19.06. Found: C, 72.02; H, 4.54; N, 18.94.

4.1.6.3 5,8-Dimethyl-3-phenyl-3H-[1,2,3]triazolo[4,5-*h*][1,6]naphthyridine (5d)

This compound was obtained from reaction of **23a** with acetone. White solid; yield: 56%; mp: 190.0-190.5 °C; ¹H NMR (200 MHz, CDCl₃) δ: 2.94 (3H, s, CH₃), 3.08 (3H, s, CH₃), 7.50-7.67 (4H, m, ArH), 8.33-8.48 (3H, m, ArH); ¹³C NMR (50 MHz, CDCl₃) δ: 23.0 (q), 28.2 (q), 119.0 (s), 122.1 (2 x d), 122.8 (d), 128.4 (d), 129.4 (2 x d), 133.1 (s), 135.1 (d), 136.6 (s), 143.7 (s),

143.8 (s), 162.2 (s), 165.4 (s). Anal. Calcd for C₁₆H₁₃N₅: C, 69.80; H, 4.76; N, 25.44. Found: C, 69.64; H, 4.93; N, 25.52.

4.1.6.4 8-(2-Methoxyphenyl)-3-(4-methoxyphenyl)-5-methyl-3*H*-[1,2,3]triazolo[4,5-*h*][1,6]naphthyridine (5f)

This compound was obtained from reaction of **23b** with 2-methoxy-acetophenone. White solid; yield: 55%; mp: 215.1-215.4 °C; ¹H NMR (200 MHz, CDCl₃) δ: 3.09 (3H, s, CH₃), 3.91 (3H, s, CH₃O), 3.93 (3H, s, CH₃O), 7.04-7.23 (4H, m, ArH), 7.44-7.53 (1H, m, ArH), 8.17-8.31 (4H, m, ArH), 8.53 (1H, d, *J* = 8.8 Hz, H₆); ¹³C NMR (50 MHz, CDCl₃) δ: 23.1 (q), 55.6 (q), 55.7 (q), 111.4 (d), 114.6 (2 x d), 119.3 (s), 121.4 (d), 123.9 (2 x d), 124.2 (d), 128.0 (s), 129.7 (s), 131.5 (d), 132.7 (d), 133.2 (s), 134.3 (d), 143.7 (s), 144.1 (s), 157.6 (s), 159.6 (s), 161.6 (s), 161.9 (s). Anal. Calcd for C₂₃H₁₉N₅O₂: C, 69.51; H, 4.82; N, 17.62. Found: C, 69.62; H, 4.74; N, 17.43.

4.1.6.5 3,8-Bis(4-methoxyphenyl)-5-methyl-3*H*-[1,2,3]triazolo[4,5-*h*][1,6]naphthyridine (5g)

This compound was obtained from reaction of **23b** with 4-methoxy-acetophenone. White solid; yield: 60%; mp: 238.9-239.6 °C; ¹H NMR (200 MHz, CDCl₃) δ: 3.06 (3H, s, CH₃), 3.91 (3H, s, CH₃O), 3.92 (3H, s, CH₃O), 7.06-7.15 (4H, m, ArH), 8.04 (1H, d, *J* = 8.8 Hz, H₇), 8.18 (2H, d, *J* = 9.0 Hz, ArH), 8.40 (2H, d, *J* = 9.0 Hz, ArH), 8.53 (1H, d, *J* = 8.8 Hz, H₆); ¹³C NMR (50 MHz, CDCl₃) δ: 23.1 (q), 55.5 (q), 55.6 (q), 114.3 (2 x d), 114.6 (2 x d), 118.5 (d), 119.2 (s), 123.9 (2 x d), 129.7 (s), 129.8 (2 x d), 130.5 (s), 133.2 (s), 135.7 (d), 143.9 (s), 144.3 (s), 159.6 (s), 161.2 (s), 161.9 (2 x s). Anal. Calcd for C₂₃H₁₉N₅O₂: C, 69.51; H, 4.82; N, 17.62. Found: C, 69.45; H, 4.93; N, 17.78.

4.1.6.6 3-(4-Methoxyphenyl)-5,8-dimethyl-3*H*-[1,2,3]triazolo[4,5-*h*][1,6]naphthyridine (5h)

This compound was obtained from reaction of **23b** with acetone. Light yellow solid; yield: 44%; mp: 228.0-229.1 °C; ¹H NMR (200 MHz, CDCl₃) δ: 2.91 (3H, s, CH₃), 3.03 (3H, s, CH₃), 3.90 (3H, s, CH₃O), 7.11 (2H, d, *J* = 9.0 Hz, H₂' and H₆'), 7.48 (1H, d, *J* = 8.6 Hz, H₇'), 8.18 (2H, d, *J* = 9.0 Hz, H₃' and H₅'), 8.40 (1H, d, *J* = 8.6 Hz, H₆); ¹³C NMR (50 MHz, CDCl₃) δ: 23.0 (q), 25.7 (q), 55.6 (q), 114.5 (2 x d), 118.9 (s), 122.7 (d), 123.7 (2 x d), 129.7 (s), 132.8 (s), 135.0 (d), 143.5 (s), 143.7 (s), 159.6 (s), 161.9 (s), 165.2 (s). Anal. Calcd for C₁₇H₁₅N₅O: C, 66.87; H, 4.95; N, 22.94. Found: C, 66.79; H, 5.03; N, 23.11.

4.1.6.7 5-Methyl-8-phenyl-3-(3,4,5-trimethoxyphenyl)-3*H*-[1,2,3]triazolo[4,5-*h*][1,6]naphthyridine (**5i**)

This compound was obtained from reaction of **23c** with acetophenone. White solid; yield: 60%; mp: 212.7-213.0 °C; ¹H NMR (200 MHz, CDCl₃) δ: 3.12 (3H, s, CH₃), 3.95 (3H, s, CH₃O), 4.02 (6H, s, CH₃Ox2), 7.57-7.60 (3H, m, ArH), 7.69 (2H, s, H₂' and H₆'), 8.14 (1H, d, *J* = 8.8 Hz, H₇'), 8.40-8.45 (2H, m, ArH), 8.63 (1H, d, *J* = 8.8 Hz, H₆); ¹³C NMR (50 MHz, CDCl₃) δ: 23.3 (q), 56.4 (2 x q), 61.1 (q), 100.0 (2 x d), 119.3 (d), 119.6 (s), 128.3 (2 x d), 129.0 (2 x d), 131.0 (d), 132.4 (s), 133.5 (s), 135.9 (d), 137.9 (2 x s), 143.9 (s), 144.2 (s), 153.7 (2 x s), 162.0 (s), 162.1 (s). Anal. Calcd for C₂₄H₂₁N₅O₃: C, 67.44; H, 4.95; N, 16.38. Found: C, 67.57; H, 4.82; N, 16.23.

4.1.6.8 8-(2-Methoxyphenyl)-5-methyl-3-(3,4,5-trimethoxyphenyl)-3*H*-[1,2,3]triazolo[4,5-*h*][1,6]naphthyridine (**5j**)

This compound was obtained from reaction of **23c** with 2-methoxy-acetophenone. White solid; yield: 55%; mp: 210.5-211.7 °C; ¹H NMR (200 MHz, CDCl₃) δ: 3.11 (3H, s, CH₃), 3.93 (3H, s, CH₃O), 3.94 (3H, s, CH₃O), 4.02 (6H, s, 2 x CH₃O), 7.07 (1H, d, *J* = 8.8 Hz, H₇'), 7.16-7.24 (1H, m, ArH), 7.46-7.54 (1H, m, ArH), 7.69 (2H, s, H₂' and H₆'), 8.28- 8.32 (2H, m, ArH), 8.55 (1H, d,

$J = 8.8$ Hz, H_6); ^{13}C NMR (50 MHz, CDCl_3) δ : 23.3 (q), 55.7 (q), 56.4 (2 x q), 61.1 (q), 99.7 (2 x d), 111.4 (d), 119.3 (s), 121.5 (d), 124.3 (d), 127.9 (s), 131.6 (d), 132.4 (s), 132.7 (d), 133.5 (s), 134.3 (d), 137.9 (s), 143.7 (s), 144.1 (s), 153.7 (2 x s), 157.6 (s), 161.8 (s), 162.1 (s). Anal. Calcd for $\text{C}_{25}\text{H}_{23}\text{N}_5\text{O}_4$: C, 65.63; H, 5.07; N, 15.31. Found: C, 65.72; H, 4.92; N, 15.23.

4.1.6.9 8-(2-Methoxyphenyl)-5-methyl-2-phenyl[1,3]oxazolo[5,4-*h*][1,6]naphthyridine (6b)

This compound was obtained from reaction of **24a** with 2-methoxy-acetophenone. Yellow solid; yield: 58%; mp: 221.9-222.3 °C; ^1H NMR (200 MHz, CDCl_3) δ : 3.09 (3H, s, CH_3), 3.91 (3H, s, CH_3O), 7.06 (1H, d, $J = 7.5$ Hz, ArH), 7.18 (1H, t, $J = 7.5$ Hz, ArH), 7.44 -7.56 (4H, m, ArH), 8.12-8.18 (2H, m, ArH), 8.39-8.43 (2H, m, ArH), 8.52 (1H, d, $J = 9.0$ Hz, H_6); ^{13}C NMR (50 MHz, CDCl_3) δ : 22.3 (q), 55.7 (q), 111.4 (d), 120.1 (s), 121.4 (d), 123.6 (d), 127.1 (2 x s), 127.7 (2 x d), 128.5 (s), 128.9 (2 x d), 131.4 (d), 131.5 (d), 132.5 (d), 134.2 (d), 144.6 (s), 156.0 (s), 157.5 (s), 157.6 (s), 161.3 (s), 161.7 (s). Anal. Calcd. for $\text{C}_{23}\text{H}_{17}\text{N}_3\text{O}_2$: C, 75.19; H, 4.66; N, 11.44. Found: C, 75.05; H, 4.51; N, 11.62.

4.1.6.10 5,8-Dimethyl-2-phenyl[1,3]oxazolo[5,4-*h*][1,6]naphthyridine (6d)

This compound was obtained from reaction of **24a** with acetone. Yellow solid; yield: 40%; mp: 199.6-200.3 °C; ^1H NMR (200 MHz, CDCl_3) δ : 2.92 (3H, s, CH_3), 3.05 (3H, s, CH_3), 7.43-7.57 (4H, m, ArH), 8.40-8.46 (3H, m, ArH); ^{13}C NMR (50 MHz, CDCl_3) δ : 22.1 (q), 25.9 (q), 119.7 (s), 122.1 (d), 126.6 (s), 127.0 (s), 127.7 (2 x d), 128.9 (2 x d), 131.6 (d), 135.1 (d), 144.3 (s), 156.0 (s), 157.7 (s), 161.4 (s), 164.9 (s). Anal. Calcd. $\text{C}_{17}\text{H}_{13}\text{N}_3\text{O}$: C, 74.17; H, 4.76; N, 15.26. Found: C, 74.03; H, 4.92; N, 15.44.

4.1.6.11 2-(4-Methoxyphenyl)-5-methyl-8-phenyl[1,3]oxazolo[5,4-*h*][1,6]naphthyridine (6e)

This compound was obtained from reaction of **24b** with acetophenone. Yellow solid; yield: 42%; mp: 247.3-248.4 °C; ^1H NMR (200 MHz, CDCl_3) δ : 3.05 (3H, s, CH_3), 3.90 (3H, s, CH_3O), 7.05

(2H, d, $J = 9.0$ Hz, ArH), 7.53-7.59 (3H, m, ArH), 7.99 (1H, d, $J = 9.0$, H₇), 8.32-8.37 (4H, m, ArH), 8.55 (1H, d, $J = 9.0$ Hz, H₆); ¹³C NMR (50 MHz, CDCl₃) δ : 22.1 (q), 55.5 (q), 114.4 (2 x d), 118.5 (d), 119.5 (s), 120.1 (s), 127.1 (s), 128.2 (2 x d), 128.8 (2 x d), 129.5 (2 x d), 130.5 (d), 135.9 (d), 138.2 (s), 144.4 (s), 155.3 (s), 157.8 (s), 161.3 (s), 161.6 (s), 162.4 (s). Anal. Calcd. C₂₃H₁₇N₃O₂: C, 75.19; H, 4.66; N, 11.44. Found: C, 75.00; H, 4.83; N, 11.56.

4.1.6.12 2-(4-Methoxyphenyl)-5,8-dimethyl[1,3]oxazolo[5,4-*h*][1,6]naphthyridine (6h)

This compound was obtained from reaction of **24b** with acetone. Yellow solid; yield: 48%; mp: 187.3-188.5 °C; ¹H NMR (200 MHz, CDCl₃) δ : 2.90 (3H, s, CH₃), 3.03 (3H, s, CH₃), 3.90 (3H, s, CH₃O), 7.04 (2H, d, $J = 9.0$ Hz, H_{3'} and H_{5'}), 7.42 (1H, d, $J = 8.7$ Hz, H₇), 8.34-8.43 (3H, m, H₂, H_{6'} and H₆); ¹³C NMR (50 MHz, CDCl₃) δ : 22.1 (q), 25.9 (q), 55.5 (q), 114.4 (2 x d), 119.5 (s), 119.6 (s), 122.0 (d), 126.6 (s), 129.5 (2 x d), 135.1 (d), 144.0 (s), 155.2 (s), 157.6 (s), 161.6 (s), 162.4 (s), 164.7 (s). Anal. Calcd. for C₁₈H₁₅N₃O₂: C, 70.81; H, 4.95; N, 13.76. Found: C, 71.09; H, 5.13; N, 13.52.

4.1.6.13 5-Methyl-8-phenyl-2-(3,4,5-trimethoxyphenyl)[1,3]oxazolo[5,4-*h*][1,6]naphthyridine (6i)

This compound was obtained from reaction of **24c** with acetophenone. Yellow solid; yield: 45%; mp: 229.1-229.9 °C; ¹H NMR (200 MHz, CDCl₃) δ : 3.05 (3H, s, CH₃), 3.96 (3H, s, CH₃O), 4.00 (6H, s, 2 x CH₃O), 7.52-7.59 (3H, m, H_{3''}, H_{4''} and H_{5''}), 7.65 (2H, s, H_{2''} and H_{6''}), 8.00 (1H, d, $J=8.9$ Hz, H₇), 8.31-8.36 (2H, m, H_{2''} and H_{6''}), 8.56 (1H, d, $J=8.9$ Hz, H₆); ¹³C NMR (50 MHz, CDCl₃) δ : 22.2 (q), 56.4 (2 x q), 61.0 (q), 104.7 (2 x d), 118.7 (d), 120.3 (s), 121.9 (s), 127.1 (s), 128.2 (2 x d), 128.9 (2 x d), 130.5 (d), 136.0 (d), 138.2 (s), 140.9 (s), 144.4 (s), 153.5 (2 x s), 155.9 (s), 157.8 (s), 161.2 (s), 161.6 (s). Anal. Calcd for C₂₅H₂₁N₃O₄: C, 70.25; H, 4.95; N, 9.83. Found: C, 70.49; H, 4.72; N, 9.74.

4.1.6.14 8-(2-Methoxyphenyl)-5-methyl-2-(3,4,5-trimethoxyphenyl)[1,3]oxazolo[5,4-*h*][1,6]naphthyridine (6j)

This compound was obtained from reaction of **24c** with 2-methoxy-acetophenone. Yellow solid; yield: 56%; mp: 191.7-192.0 °C; ¹H NMR (200 MHz, CDCl₃) δ: 3.09 (3H, s, CH₃), 3.91 (3H, s, CH₃O), 3.95 (3H, s, CH₃O), 4.00 (6H, s, 2 x CH₃O), 7.06 (1H, d, *J* = 8.2, ArH), 7.18 (1H, t, *J* = 8.2 Hz, ArH), 7.48 (1H, t, *J* = 8.2 Hz, ArH), 7.69 (2H, s, H_{2'} and H_{6'}), 8.14 (2H, d, *J* = 8.9 Hz, ArH), 8.54 (1H, d, *J* = 9.0 Hz, H₆); ¹³C NMR (50 MHz, CDCl₃) δ: 22.2 (q), 55.7 (q), 56.4 (2 x q), 61.0 (q), 104.7 (2 x d), 111.4 (d), 120.1 (s), 121.4 (d), 122.1 (s), 123.6 (d), 127.1 (s), 128.5 (s), 131.4 (d), 132.4 (d), 134.2 (d), 140.9 (s), 144.5 (s), 153.5 (2 x s), 155.8 (s), 157.5 (s), 157.6 (s), 161.2 (s), 161.7 (s). Anal. Calcd. for C₂₆H₂₃N₃O₅: C, 68.26; H, 5.07; N, 9.19. Found: C, 68.35; H, 5.25; N, 9.01.

4.1.6.15 5,8-Dimethyl-2-(3,4,5-trimethoxyphenyl)[1,3]oxazolo[5,4-*h*][1,6]naphthyridine (6l)

This compound was obtained from reaction of **24c** with acetone. White solid; yield: 40%; mp: 151.7-152.1 °C; ¹H NMR (200 MHz, CDCl₃) δ: 2.93 (3H, s, CH₃), 3.06 (3H, s, CH₃), 3.95, (3H, s, CH₃O), 4.00 (6H, s, 2 x CH₃O), 7.46 (1H, d, *J* = 8.7 Hz, H₇), 7.69, (2H, s, H_{2'} and H_{6'}), 8.45 (1H, d, *J* = 8.7 Hz, H₆); ¹³C NMR (50 MHz, CDCl₃) δ: 22.2 (q), 25.9 (q), 56.4 (2 x q), 61.1 (q), 104.8 (2 x d), 119.8 (s), 122.0 (s), 122.2 (d), 126.7 (s), 135.2 (d), 141.0 (s), 144.2 (s), 153.5 (2 x s), 155.8 (s), 157.6 (s), 161.2 (s), 164.9 (s). Anal. Calcd. for C₂₀H₁₉N₃O₄: C, 65.74; H, 5.24; N, 11.50. Found: C, 65.97; H, 5.02; N, 11.24.

4.1.7 General Procedure for the Synthesis of 5-Methyl-3-substituted-3,9-dihydro-8*H*-[1,2,3]triazolo[4,5-*h*][1,6]naphthyridin-8-one derivatives (7a-c) and 5-Methyl-2-substituted[1,3]oxazolo[5,4-*h*][1,6]naphthyridin-8(9*H*)-one derivatives (8a-c)

To a suspension of 7-amino-5-methyl-2-substituted-[1,2,3]triazolo[5,4-*b*]pyridine-6-carbaldehyde derivative **23a-c** (0.42 mmol) or 7-amino-5-methyl-2-substituted-[1,3]oxazolo[5,4-*b*]pyridine-6-carbaldehyde derivatives **24a-c** (0.42 mmol) in anhydrous ethanol (10 mL), potassium carbonate (1.26 mmol) was added at room temperature. The reaction mixture was stirred for few minutes and then triethyl phosphonoacetate (0.25 mL, 1.26 mmol) was added. The reaction mixture was refluxed for 12 h. The solvent was removed under reduced pressure and ice and water were added (50 mL). The precipitate was filtered off, dried and purified by chromatography (DCM/AcOEt 8/2). The poor solubility of compounds **7a-c** and **8a-c** prevented ^{13}C NMR spectra from being recorded.

4.1.7.1 5-Methyl-3-phenyl-3,9-dihydro-8*H*-[1,2,3]triazolo[4,5-*h*][1,6]naphthyridin-8-one (7a)

This compound was obtained from reaction of **23a**. Light yellow solid; yield: 60%; mp: 304.5-305 °C; IR cm^{-1} : 3610 (NH), 1675 (CO); ^1H NMR (200 MHz, DMSO- d_6) δ : 2.87 (3H, s, CH₃), 6.65 (1H, d, J = 10.0 Hz, H₇), 7.57-7.74 (3H, m, ArH and H₆), 8.18-8.32 (3H, m, ArH), 13.26 (1H, s, NH). Anal. Calcd for C₁₅H₁₁N₅O: C, 64.97; H, 4.00; N, 25.26. Found: C, 64.77; H, 4.15; N, 25.38.

4.1.7.2 3-(4-Methoxyphenyl)-5-methyl-3,9-dihydro-8*H*-[1,2,3]triazolo[4,5-*h*][1,6]naphthyridin-8-one (7b)

This compound was obtained from reaction of **23b**. Yellow solid; yield: 55%; mp: 279.1-280.0 °C; IR cm^{-1} : 3421 (NH), 1669 (CO); ^1H NMR (200 MHz, DMSO- d_6) δ : 2.80 (3H, s, CH₃), 3.87 (3H, s, CH₃O), 6.53 (1H, d, J = 10.0 Hz, H₇), 7.23 (2H, d, J = 8.0 Hz H_{2'} and H_{6'}), 8.06 (3H, m, H_{3'}, H_{5'} and H₆), 13.24 (1H, s, NH). Anal. Calcd for C₁₆H₁₃N₅O₂: C, 62.53; H, 4.26; N, 22.79. Found: C, 62.65; H, 4.21; N, 22.65.

4.1.7.3 5-Methyl-2-phenyl[1,3]oxazolo[5,4-*h*][1,6]naphthyridin-8(9*H*)-one (8a)

This compound was obtained from reaction of **24a**. White solid; yield: 45%; mp: 199.4-200.5 °C; IR cm^{-1} : 3400 (NH), 1630 (CO); $^1\text{H NMR}$ (200 MHz, CDCl_3) δ : 2.88 (3H, s, CH_3), 6.72 (1H, d, $J = 10.0$ Hz, H_7), 7.54-7.65 (3H, m, H_3 , H_4 and H_5), 8.07 (1H, d, $J = 10.0$ Hz, H_6), 8.22-8.26 (2H, m, H_2 and H_6), 9.98 (1H, s, NH). Anal. Calcd. for $\text{C}_{16}\text{H}_{11}\text{N}_3\text{O}_2$: C, 69.31; H, 4.00; N, 15.15. Found: C, 69.20; H, 4.12; N, 15.34.

4.2. Photophysical characterization and photooxidation study

4.2.1 Photophysical characterization

All spectrophotometric measures were performed using UV-Vis Perkin Elmer instrument (Lambda 25). For all the compounds, absorption spectra, molar extinction coefficients (ϵ) and determination of maxima peaks (λ_{max}) were carried out in 20 mM PB, pH 7.4. The emission spectra of the compound **6e** was performed on Cary Eclipse Fluorescence Spectrophotometer. All spectrometers were equipped with Peltier temperature controllers. Quartz cuvettes of 0.4-10 cm path length were used.

4.2.2. Fluorescence quantum yield measurement

Fluorescence quantum yield values for the compound **6e** were obtained using 3-hydroxyflavone as primary reference ($\phi = 0.2$ in chloroform and 0.035 in ethanol [59]). Fluorescent emission was measured exciting the compounds at three different excitation wavelengths (335, 340 and 344 nm) and integrating the resulting spectrum between 360 and 650nm. Φ values were calculated applying the following formula:

$$\varphi_{\text{sample}} = \varphi_{\text{reference}} * \frac{\text{Area}_{\text{sample}}}{\text{Area}_{\text{reference}}} * \frac{\text{Abs}_{\text{reference}}}{\text{Abs}_{\text{sample}}} * \frac{\eta_{\text{sample}}^2}{\eta_{\text{reference}}^2}$$

Where *Area* is the area subtended by the curve, *Abs* is the absorption value at the excitation wavelength and η is the refractive index of the solution. All data are presented as a mean of the values obtained at the three wavelengths and are the average of three replicates.

4.2.3. Spectroscopic and kinetic characterization of the triplet excited state, by LFP

LP 920 Edinburgh Instrument photolysis system has been employed to carry out all the detection experiments of the transient species. The minimum response time of the detection system was of about 10 ns. The laser beam (a Nd/YAG operated at $\lambda = 355$ nm) was focused on a 3 mm wide circular area of the cell and the first 5 mm in depth were analyzed at a right angle geometry. The incident pulse energies used were 30 mJ per pulse. The spectra were reconstructed point from time profiles taken each 5 nm. The absorbance at 355 nm A_{355} was ~ 1.0 over 1 cm. Ar-saturated or air-equilibrated solutions were used. The sample was renewed after few laser shots. Temperature was 295 K.

4.2.4. Generation of $^1\text{O}_2$ and its trapping by 9,10-anthracenedipropionic acid in aqueous acetonitrile

Quantum yield measurements for ADPA consumption (ϕ_R) were measured by irradiating 2 mL $2.5 \cdot 10^{-5}$ M of **6e** and **5h** (acetonitrile: water = 3:2 solutions) in 1cm optical path cuvettes in the presence of $1.1 \cdot 10^{-4}$ M concentration of ADPA, after flushing with oxygen. The lamp source was a focalized 150 W high-pressure mercury arc fitted with a transmittance filter (transmission 400 nm). Potassium ferrioxalate was used as the actinometer. [60,61]

4.3 Biology

4.3.1 Compound solubilization in DMSO

[1,2,3]Triazolo[4,5-*h*][1,6]naphthyridines **5a-1**, [1,3]oxazolo[5,4-*h*][1,6]naphthyridines **6a-1**, and [1,2,3]triazolo[4,5-*h*][1,6]naphthyridin-8-ones **7a-c**, [1,3]oxazolo[5,4-*h*][1,6]naphthyridin-8-ones **8a-c** were resuspended in dimethyl sulfoxide (DMSO), which was chosen among organic solvents as it can be administered to human cell lines in small percentage without induction of cytotoxicity. Since within each series of compounds, some derivatives showed solubility issues, further studies were conducted only on compounds that completely dissolved and were stable in DMSO.

4.3.2 Irradiation procedures

Irradiation experiments were performed in a photochemical multirays reactor, equipped with 10 UV lamps (3660 Å), emitting at 365 nm (Helios Italquartz, Italy). The spectral irradiance of the source was 5 mw/cm² as measured with a UVX Radiometer (UVP, Upland, CA, USA).

4.3.3 Cellular cytotoxicity and phototoxicity

Cytotoxic effects were determined by MTT assay. Derivatives reported in Table 4 were dissolved and diluted into working concentrations with DMSO. All cell lines were grown and maintained according to manufacturer's instructions (<https://www.lgcstandards-atcc.org>). Cells were plated into 96-microwell plates to a final volume of 100 µL and allowed an overnight period for attachment. The following day, the tested compounds were added to each well to reach a 0.5% final concentration of DMSO per well; each concentration was tested in triplicate. Compounds were incubated for 5 min, then cells were washed in 1x PBS (100 µL) and fresh

medium was added. In phototoxicity experiments, immediately after medium removal, cells were irradiated on ice for 5 min at 365 nm, corresponding to 1.5 J/cm^2 , in a photochemical multirays reactor and incubated at $37 \text{ }^\circ\text{C}$ for 72 h. Control cells (without any compound but with 0.5% DMSO) were treated in the exact same conditions. Cell survival was evaluated by MTT assay: 10 μL of freshly dissolved solution of MTT (5 mg/mL in PBS) were added to each well, and after 4 h of incubation, MTT crystals were solubilized in solubilization solution (10% sodium dodecyl sulphate (SDS) and 0.01 M HCl). After overnight incubation at $37 \text{ }^\circ\text{C}$, absorbance was read at 540 nm. Data were expressed as mean values of at least three individual experiments conducted in triplicate. The percentage of cell survival was calculated as follows: cell survival = $(A_{\text{well}} - A_{\text{blank}})/(A_{\text{control}} - A_{\text{blank}}) \times 100$, where blank denotes the medium without cells. Each experiment was repeated at least three times.

4.3.4 Reactive oxygen species (ROS) detection in cells

The cell-permeant 2',7'-dichlorodihydrofluorescein diacetate (H_2DCFDA) is a chemically reduced form of fluorescein used as an indicator for reactive oxygen species (ROS) in cells. Oxidation results in the formation of fluorescent DCF, which is maximally excited at 495 nm and emits at 520 nm. MCF7 cells (3×10^4) were plated in 96 wells plates medium 24 h before the assay was performed, so that cells reached 80–90% of confluence on the day of the experiment. RPMI medium containing 10% FBS was removed and compounds were incubated at different concentrations for 30 min in phenol red and serum free medium to avoid subsequent probe oxidation. H_2DCFDA probe (10 μM) was added to cell medium and incubated for 15 minutes prior to irradiation (1.5 J/cm^2). Control plates that did not undergo irradiation were also included in each experiment. NAC (N-acetyl-L-cysteine) was used as antioxidant control compound; NAC prevention of ROS formation was performed at different concentrations. Phorbol-12-

myristate-13-acetate (PMA) was used as a validated ROS-inducer compound. ROS production was monitored at Victor X2 Multilabel plate reader, lamp filter 485 nm and emission filter 535 nm (Perkin Elmer Italia, Milan).

4.3.5 Flow cytometry

For cell cycle distribution analysis only adherent cells were fixed in 70% EtOH and incubated at 4 °C for 30 min in staining solution containing 50 µg/mL of propidium iodide, 50 mg/mL of RNase, and 0.05% Igepal in PBS. Samples (at least 30000 events) were analyzed on an LRS 2 instrument using FACS DIVA Software (BD Bioscience) and analyzed with Flow Jo (Tree Star). The rate of apoptotic cells was measured by the amount of cell surface exposure of phosphatidylserine. MCF7 cells in exponential growth were treated with different concentrations of the test compounds for 4 h. Cells were pelleted, washed in 1x PBS and stained with FITC annexin V according to the manufacturer's instructions (Annexin V-FITC Apoptosis Detection Kit, eBioscience, Thermo Fisher Scientific Inc.). Subsequently, cells were counterstained with propidium iodide (PI), according to the manufacturer's instructions (Annexin V-FITC Apoptosis Detection Kit, eBioscience, Thermo Fisher Scientific Inc.). Samples were analyzed on an LRS 2 instrument using FACS DIVA Software (BD Bioscience) and analyzed with Flow Jo (Tree Star).

4.3.6 Confocal imaging

For confocal imaging cells were seeded on glass cover-slips 24 h prior compound administration. Cells were washed in 1x PBS, fixed in paraformaldehyde (PFA, 2%) and mounted in Vectashield mounting medium (DBA ITALIA, Milan, Italy). Images were captured at a Leica SP2 or SP5 confocal microscope (63x objective, Green HeNe (Helium Neon) laser λ_{ex} 543 nm, λ_{em} 560-620 nm, Blue Argon laser λ_{ex} 488 nm, λ_{em} 500-530 nm and 405 diode laser λ_{ex} 405 nm, λ_{em} 415-460 nm).

4.3.7 Analysis of mitochondrial dysfunction by confocal microscopy

Mitochondria were labelled in live-cells using Mitotracker Orange CMTM-ROS (Thermo Fisher Scientific, Milan, Italy). MCF7 cells were plated on glass slides (4×10^5). After 24 h the complete medium was removed and replaced with phenol red and serum free medium containing the mitochondrial probe (150 nM), the probe was incubated 45 min prior to addition of compounds and photoactivation. After irradiation cells were washed in 1x PBS, fixed in paraformaldehyde (PFA, 2%) and mounted in Vectashield mounting medium (DBA ITALIA, Milan, Italy). Nuclei were stained with Nuclear Green dye LCS1 (Abcam, λ_{ex} 503 nm, λ_{em} 526 nm). Phorbol-12-myristate-13-acetate (PMA) was used as a validated ROS-inducer compound. Images were captured at a Leica SP2 confocal microscope (63x objective, Green HeNe (Helium Neon) laser λ_{ex} 543 nm, λ_{em} 560-620 nm and the Blue Argon laser λ_{ex} 488 nm, λ_{em} 500-530 nm for the nuclear staining).

4.3.8 Analysis of lysosomal activation by confocal microscopy

Lysosomes were labelled in live-cells using LysoTracker Green DND 26 (Thermo Fisher Scientific, Milan, Italy). MCF7 cells were plated on glass slides (4×10^5). After 24 h the complete medium was removed and replaced with phenol red and serum free medium containing the mitochondrial probe (175 nM), the probe was incubated 45 min prior to addition of compounds and photoactivation. After irradiation cells were washed in 1x PBS, fixed in paraformaldehyde (PFA, 2%) and mounted in Vectashield mounting medium (DBA ITALIA, Milan, Italy). Phorbol-12-myristate-13-acetate (PMA) was used as a validated ROS-inducer compound.

Images were captured at a Leica SP2 confocal microscope (63x objective, Blue Argon laser λ_{ex} 488 nm, λ_{em} 500-530 nm for the nuclear staining).

4.3.9 Statistical Analysis.

Pairwise comparisons between means of different groups and experiments were performed using a Student t-test (two tailed, unpaired, unpaired) where, for each couple of normally distributed populations (i.e. treated vs untreated), the null hypothesis that the means are equal was verified. The difference between two subsets of data was considered statistically significant if the Student t-test gives a significance level P (P value) less than 0.01.

Corresponding Author Information:

*Phone: +39-091-23896826. E-mail: alessandra.montalbano@unipa.it.

*Phone: +39-049-8272346. E-mail: sara.richter@unipd.it

Author Contributions:

I. F. and V.S. contributed equally to this work. A.M. and S.R. share senior authorship.

Acknowledgment:

This work was financially supported by Ministero dell'Istruzione dell'Università e della Ricerca (MIUR).

Abbreviations Used:

PMA, phorbol-12-myristate-13-acetate

SI, selectivity index

PTI, phototoxicity index

ROS, reactive oxygen species

EC₅₀: effective concentration (able to kill 50% of cell population)

CC₅₀: cytotoxic concentration (able to kill 50% of cell population)

References

- [1] Litvinov, V. P.; Roman, S. V.; Dyachenko, V. D. Pyridopyridines. *Russ. Chem. Rev.*, **2001**, *70*, 299-320.
- [2] Mishio, S.; Hirose, T.; Minamida, A.; Matsumoto, J.; Minami, S. Pyridonecarboxylic acid as antibacterial agents. V. Synthesis of 1-vinyl-1,4-dihydro-4-oxo-1,8- and 1,6-naphthyridine-3-carboxylic acids. *Chem. Pharm. Bull.*, **1985**, *33*, 4402-4408.
- [3] White, R. E.; Demuth, T. P. Process for making antimicrobial quinolonyl lactams. US Patent 5,281,703, Jan 25, 1994.
- [4] Austin, N. E.; Hadley, M. S.; Harling, J. D.; Harrington, F. P.; Macdonald G. J.; Mitchell, D. J.; Riley, G. J.; Stean, T. O.; Stemp, G.; Stratton, S. C.; Thomson, M.; Upton, N. The design of 8,8-dimethyl[1,6]naphthyridines as potential anticonvulsant agents. *Bioorg. Med. Chem. Lett.*, **2003**, *13*, 1627-1629.
- [5] Chan, L.; Jin, H.; Stefanac, T.; Lavallée, J.-F.; Falardeau, G.; Wang, W.; Bédard, J.; May, S.; Yuen, L. Discovery of 1,6-naphthyridines as a novel class of potent and selective human cytomegalovirus inhibitors. *J. Med. Chem.*, **1999**, *42*, 3023-3025.

- [6] Chan, L.; Stefanac, T.; Lavallée, J.-F.; Haolun, J.; Bédard, J.; May, S.; Falardeau, G. Design and synthesis of new potent human cytomegalovirus (HCMV) inhibitors based on internally hydrogen-bonded 1,6-naphthyridines. *Bioorg. Med. Chem. Lett.*, **2001**, *11*, 103-105.
- [7] Falardeau, G.; Lachance, H.; St-Pierre, A.; Yannopoulos, C. G.; Drouin, M.; Bédard, J.; Chan, L. Design and synthesis of potent macrocyclic 1,6-naphthyridine anti-human cytomegalovirus (HCMV) inhibitors. *Bioorg. Med. Chem. Lett.*, **2005**, *15*, 1693-1695.
- [8] Zhuang, L.; Wai, J. S.; Embrey, M. W.; Fisher, T. E.; Egbertson, M. S.; Payne, L. S.; Guare, J. P.; Vacca, J. P.; Hazuda, D. J.; Felock, P. J.; Wolfe, A. L.; Stillmock, K. A.; Witmer, M. V.; Moyer, G.; Schleif, W. A.; Gabryelski, L. J.; Leonard, Y. M.; Lynch, J. J.; Michelson, S. R.; Young, S. D. Design and synthesis of 8-hydroxy-[1,6]naphthyridines as novel inhibitors of HIV-1 integrase in vitro and in infected cells. *J. Med. Chem.*, **2003**, *46*, 453-456.
- [9] Embrey, M. W.; Wai, J. S.; Funk, T. W.; Homnick, C. F.; Perlow, D. S.; Young, S. D.; Vacca, J. P.; Hazuda, D. J.; Felock, P. J.; Stillmock, K. A.; Witmer, M. V.; Moyer, G.; Schleif, W. A.; Gabryelski, L. J.; Jin, L.; Chen, I.-W.; Ellis, J. D.; Wong, B. K.; Lin, J. H.; Leonard, Y. M.; Tsou, N. N.; Zhuang, L. A series of 5-(5,6)-dihydrouracil substituted 8-hydroxy-[1,6]naphthyridine-7-carboxylic acid 4-fluorobenzylamide inhibitors of HIV-1 integrase and viral replication in cells. *Bioorg. Med. Chem. Lett.*, **2005**, *15*, 4550-4554.
- [10] Zeng, L.-F.; Wang, Y.; Kazemi, R.; Xu, S.; Xu, Z.-L.; Sanchez, T. W.; Yang, L.-M.; Debnath, B.; Odde, S.; Xie, H.; Zheng, Y.-T.; Ding, J.; Neamati, N.; Long, Y.-Q. Repositioning HIV-1 integrase inhibitors for cancer therapeutics: 1,6-naphthyridine-7-carboxamide as a promising scaffold with drug-like properties. *J. Med. Chem.*, **2012**, *55*, 9492-9509.
- [11] Thompson, A. M.; Connolly, C. J. C.; Hamby, J. M.; Boushelle, S.; Hartl, B. G.; Amar, A. M.; Kraker, A. J.; Driscoll, D. L.; Steinkampf, R. W.; Patmore, S. J.; Vincent, P. W.; Roberts,

- B. J.; Elliott, W. L.; Klohs, W.; Leopold, W. R.; Showalter, H. D. H.; Denny, W. A. 3-(3,5-Dimethoxyphenyl)-1,6-naphthyridine-2,7-diamines and related 2-urea derivatives are potent and selective inhibitors of the FGF receptor-1 tyrosine kinase. *J. Med. Chem.*, **2000**, *43*, 4200-4211.
- [12] Thompson, A. M.; Delaney, A. M.; Hamby, J. M.; Schroeder, M. C.; Spoon, T. A.; Crean, S. M.; Showalter, H. D. H.; Denny, W. A. Synthesis and structure–activity relationships of soluble 7-substituted 3-(3,5-dimethoxyphenyl)-1,6-naphthyridin-2-amines and related ureas as dual inhibitors of the fibroblast growth factor receptor-1 and vascular endothelial growth factor receptor-2 tyrosine kinases. *J. Med. Chem.*, **2005**, *48*, 4628-4653.
- [13] Barraja, P.; Diana, P.; Montalbano, A.; Dattolo, G.; Cirrincione, G.; Viola, G.; Vedaldi, D.; Dall’Acqua, F. Pyrrolo[2,3-*h*]quinolinones: a new ring system with potent photoantiproliferative activity. *Bioorg. Med. Chem.*, **2006**, *14*, 8712-8728.
- [14] Barraja, P.; Diana, P.; Montalbano, A.; Carbone, A.; Viola, G.; Basso, G.; Salvador, A.; Vedaldi, D.; Dall’Acqua, F.; Cirrincione, G. Pyrrolo[3,4-*h*]quinolinones a new class of photochemotherapeutic agents. *Bioorg. Med. Chem.*, **2011**, *19*, 2326-2341.
- [15] Barraja, P.; Caracausi, L.; Diana, P.; Carbone, A.; Montalbano, A.; Cirrincione, G.; Brun, P.; Palù, G.; Castagliuolo, I.; Dall’Acqua, F.; Vedaldi, D.; Salvador, A. Synthesis of pyrrolo[3,2-*h*]quinolinones with good photochemotherapeutic activity and no DNA damage. *Bioorg. Med. Chem.*, **2010**, *18*, 4830-4843.
- [16] Spanò, V.; Parrino, B.; Carbone, A.; Montalbano, A.; Salvador, A.; Brun, P.; Vedaldi, D.; Diana, P.; Cirrincione, G.; Barraja, P. Pyrazolo[3,4-*h*]quinolines promising photosensitizing agents in the treatment of cancer. *Eur. J. Med. Chem.*, **2015**, *102*, 334-351.
- [17] Spanò, V.; Frasson, I.; Giallombardo, D.; Doria, F.; Parrino, B.; Carbone, A.; Montalbano, A.; Nadai, M.; Diana, P.; Cirrincione, G.; Freccero, M.; Richter, S. N.; Barraja, P.

Synthesis and antiproliferative mechanism of action of pyrrolo[3',2':6,7]cyclohepta[1,2-*d*]pyrimidin-2-amines as singlet oxygen photosensitizers. *Eur. J. Med. Chem.*, **2016**, *123*, 447-461.

[18] Spanò, V.; Giallombardo, D.; Cilibrasi, V.; Parrino, B.; Carbone, A.; Montalbano, A.; Frasson, I.; Salvador, A.; Richter, S. N.; Doria, F.; Freccero, M.; Cascioferro, S.; Diana, P.; Cirrincione, G.; Barraja, P. Pyrrolo[3',2':6,7]cyclohepta[1,2-*b*]pyridines with potent photo-antiproliferative activity. *Eur. J. Med. Chem.*, **2017**, *128*, 300-318.

[19] Parrino, B.; Attanzio, A.; Spanò, V.; Cascioferro, S.; Montalbano, A.; Barraja, P.; Tesoriere, L.; Diana, P.; Cirrincione, G.; Carbone, A. Synthesis, antitumor activity and CDK1 inhibitor of new thiazole nortopsentin analogues. *Eur. J. Med. Chem.*, **2017**, *138*, 371-383.

[20] Parrino, B.; Ullo, S.; Attanzio, A.; Spanò, V.; Cascioferro, S.; Montalbano, A.; Barraja, P.; Tesoriere, L.; Cirrincione, G.; Diana, P. New tripentone analogs with antiproliferative activity. *Molecules*, **2017**, *22*, 2005/1-2005/13.

[21] Spanò, V.; Attanzio, A.; Cascioferro, S.; Carbone, A.; Montalbano, A.; Barraja, P.; Tesoriere, L.; Cirrincione, G.; Diana, P.; Parrino, B. Synthesis and antitumor activity of new thiazole nortopsentin analogs. *Mar. Drugs*, **2016**, *14*, 226-244.

[22] Spanò, V.; Pennati, M.; Parrino, B.; Carbone, A.; Montalbano, A.; Cilibrasi, V.; Zuco, V.; Lopercolo, A.; Cominetti, D.; Diana, P.; Cirrincione, G.; Barraja, P.; Zaffaroni, N. Preclinical activity of new [1,2]oxazolo[5,4-*e*]isoindole derivatives in diffuse malignant peritoneal mesothelioma. *J. Med. Chem.*, **2016**, *59*, 7223-7238.

[23] Barraja, P.; Spanò, V.; Giallombardo, D.; Diana, P.; Montalbano, A.; Carbone, A.; Parrino, B.; Cirrincione, G. Synthesis of [1,2]oxazolo[5,4-*e*]indazoles as antitumor agents. *Tetrahedron*, **2013**, *69*, 6474-6477.

- [24] Spanò, V.; Pennati, M.; Parrino, B.; Carbone, A.; Montalbano, A.; Lopercolo, A.; Zuco, V.; Cominetti, D.; Diana, P.; Cirrincione, G.; Zaffaroni, N.; Barraja P. [1,2]Oxazolo[5,4-*e*]isoindoles as promising tubulin polymerization inhibitors. *Eur. J. Med. Chem.*, **2016**, *24*, 840-851.
- [25] Barraja, P.; Caracausi, L.; Diana, P.; Spanò, V.; Montalbano, A.; Carbone, A.; Parrino, B.; Cirrincione, G. Synthesis and Antiproliferative Activity of the Ring System [1,2]Oxazolo[4,5-*g*]indole. *ChemMedChem*, **2012**, *7*, 1901-1904.
- [26] Carbone, A.; Parrino, B.; Di Vita, G.; Attanzio, A.; Spanò, V.; Montalbano, A.; Barraja, P.; Tesoriere, L.; Livrea, M. A.; Diana, P.; Cirrincione G. Synthesis and antiproliferative activity of thiazolyl-bis-pyrrolo[2,3-*b*]pyridines and indolyl-thiazolyl-pyrrolo[2,3-*c*]pyridines, nortopsentin analogues. *Mar. Drugs*, **2015**, *13*, 460-492.
- [27] Barraja, P.; Diana, P.; Spanò, V.; Montalbano, A.; Carbone, A.; Parrino, B.; Cirrincione, G. An efficient synthesis of pyrrolo[3',2':4,5]thiopyrano[3,2-*b*]pyridin-2-one: a new ring system of pharmaceutical interest. *Tetrahedron*, **2012**, *68*, 5087-5094.
- [28] Parrino, B.; Carbone, A.; Ciancimino, C.; Spanò, V.; Montalbano, A.; Barraja, P.; Cirrincione, G.; Diana, P.; Sissi, C.; Palumbo, M.; Pinato, O.; Pennati, M.; Beretta, G.; Folini, M.; Matyus, P.; Balogh, B.; Zaffaroni, N. Water-soluble isoindolo[2,1-*a*]quinoxalin-6-imines: In vitro antiproliferative activity and molecular mechanism(s) of action. *Eur. J. Med. Chem.*, **2015**, *94*, 149-162.
- [29] Parrino, B.; Carbone, A.; Spanò, V.; Montalbano, A.; Giallombardo, D.; Barraja, P.; Attanzio, A.; Tesoriere, L.; Sissi, C.; Palumbo, M.; Cirrincione, G.; Diana, P. Aza-isoindolo and isoindolo-azaquinoxaline derivatives with antiproliferative activity. *Eur. J. Med. Chem.*, **2015**, *94*, 367-377.

- [30] Parrino, B.; Carbone, A.; Di Vita, G.; Ciancimino, C.; Attanzio, A.; Spanò, V.; Montalbano, A.; Barraja, P.; Tesoriere, L.; Livrea, M. A.; Diana, P.; Cirrincione, G. 3-[4-(1*H*-Indol-3-yl)-1,3-thiazol-2-yl]-1*H*-pyrrolo[2,3-*b*]pyridines, nortopsentin analogues with antiproliferative activity. *Mar. Drugs*, **2015**, *13*, 1901-1924.
- [31] Parrino, B.; Ciancimino, C.; Carbone, A.; Spanò, V.; Montalbano, A.; Barraja, P.; Cirrincione, G.; Diana, P. Synthesis of isoindolo[1,4]benzoxazinone and isoindolo[1,5]benzoxazepine: two new ring systems of pharmaceutical interest. *Tetrahedron*, **2015**, *71*, 7332-7338.
- [32] Carbone, A.; Pennati, M.; Barraja, P.; Montalbano, A.; Parrino, B.; Spanò, V.; Lopercolo, A.; Sbarra, S.; Doldi, V.; Zaffaroni, N.; Cirrincione, G.; Diana, P. Synthesis and antiproliferative activity of substituted 3[2-(1*H*-indol-3-yl)-1,3-thiazol-4-yl]-1*H*-pyrrolo[3,2-*b*]pyridine, marine alkaloid nortopsentin analogues. *Curr. Med. Chem.*, **2014**, *21*, 1654-1666.
- [33] Parrino, B.; Carbone, A.; Muscarella, M.; Spanò, V.; Montalbano, A.; Barraja, P.; Salvador, A.; Vedaldi, D.; Cirrincione, G.; Diana, P. 11*H*-Pyrido[3',2':4,5]pyrrolo[3,2-*c*]cinnoline and Pyrido[3',2':4,5]pyrrolo[1,2-*c*][1,2,3]benzotriazine: two new ring systems with antitumor activity. *J. Med. Chem.*, **2014**, *57*, 9495-9511.
- [34] Parrino, B.; Spanò, V.; Carbone, A.; Barraja, P.; Diana, P.; Cirrincione, G.; Montalbano, A. Synthesis of the new ring system bispyrido[4',3':4,5]pyrrolo[1,2-*a*:1',2'-*d*]pyrazine and its deaza analogue. *Molecules*, **2014**, *19*, 13342-13357.
- [35] Spanò, V.; Montalbano, A.; Carbone, A.; Parrino, B.; Diana, P.; Cirrincione, G.; Castagliuolo, I.; Brun, P.; Issinger, O.-G.; Tisi, S.; Primac, I.; Vedaldi, D.; Salvador, A.; Barraja,

- P. Synthesis of a new class of pyrrolo[3,4-*h*]quinazolines with antimitotic activity. *Eur. J. Med. Chem.*, **2014**, *74*, 340-357.
- [36] Barraja, P.; Carbone, A.; Parrino, B.; Dall'Acqua, F.; Vedaldi, D.; Salvador, A.; Brun, P.; Castagliuolo, I.; Issinger, O. G.; Cirrincione, G. Synthesis of Triazenoazaindoles: a New Class of Triazenes with Antitumor Activity. *ChemMedChem*, **2011**, *6*, 1291-1299.
- [37] Diana, P.; Stagno, A.; Barraja, P.; Montalbano, A.; Carbone, A.; Parrino, B.; Cirrincione, G. Synthesis of the new ring system pyrrolizino[2,3-*b*]indol-4(5*H*)-one. *Tetrahedron*, **2011**, *67*, 3374-3379.
- [38] Freeman, F.; Kim, D. S. H. L. Preparation of 2-alkyl and 2-aryl-5-amino-4-cyano-1,3-oxazoles. *Tetrahedron Lett.*, **1989**, *30*, 2631-2632.
- [39] Lee, A. V.; Oesterreich, S.; Davidson, N. E. MCF-7 cells-changing the course of breast cancer research and care for 45 years. *J. Natl. Cancer Inst.*, **2015**, *107*, djv073/1-djv073/4.
- [40] Neve, R. M.; Chin, K.; Fridlyand, J.; Yeh, J.; Baehner, F. L.; Fevr, T.; Clark, L.; Bayani, N.; Coppe, J.-P.; Tong, F.; Speed, T.; Spellman, P. T.; DeVries, S.; Lapuk, A.; Wang, N. J.; Kuo, W.-L.; Stilwell, J. L.; Pinkel, D.; Albertson, D. G.; Waldman, F. M.; McCormick, F.; Dickson, R. B.; Johnson, M. D.; Lippman, M.; Ethier, S.; Gazdar, A.; Gray, J. W. A collection of breast cancer cell lines for the study of functionally distinct cancer subtypes. *Cancer Cell*, **2006**, *10*, 515-527.
- [41] Obata, T.; Mori, S.; Suzuki, Y.; Kashiwagi, T.; Tokunaga, E.; Shibata, N.; Tanaka, M. Photodynamic therapy using novel zinc phthalocyanine derivatives and a diode laser for superficial tumors in experimental animals. *J. Cancer Ther.*, **2015**, *6*, 53-61.

- [42] Jinadasa, R. G. Waruna; Hu, Xiaoke; Vicente, M. Graca H.; Smith, Kevin M. Syntheses and Cellular Investigations of 173-, 152-, and 131-Amino Acid Derivatives of Chlorin e6. *J. Med. Chem.*, 2011, *54*, 7464-7476.
- [43] Yang, N.; Weinfeld, M.; Lemieux, H.; Montpetit, B.; Goping, I. S. Photo-activation of the delocalized lipophilic cation D112 potentiates cancer selective ROS production and apoptosis. *Cell Death Dis.*, **2017**, *8*, e2587-e2600.
- [44] Doria, F.; Manet, I.; Grande, V.; Monti, S.; Freccero, M. Water-soluble naphthalene diimides as singlet oxygen sensitizers. *J. Org. Chem.*, **2013**, *78*, 8065-8073.
- [45] Traore, K.; Trush, M. A.; George, M.; Spannhake, E. W.; Anderson, W.; Asseffa, A. Signal transduction of phorbol 12-myristate 13-acetate (PMA)-induced growth inhibition of human monocytic leukemia THP-1 cells is reactive oxygen dependent. *Leuk. Res.*, *29*, **2005**, 863-879.
- [46] Keshari, R. S.; Verma, A.; Barthwal, M. K.; Dikshit, M. Reactive oxygen species-induced activation of ERK and p38 MAPK mediates PMA-induced NETs release from human neutrophils. *Cell. Biochem.*, **2013**, *114*, 532-540.
- [47] Sun, S.-Y. N-acetylcysteine, reactive oxygen species and beyond. *Cancer Biol. Ther.*, **2010**, *9*, 109-110.
- [48] Hernandez-Vargas, H.; Palacios, J.; Moreno-Bueno, G. Molecular profiling of docetaxel cytotoxicity in breast cancer cells: uncoupling of aberrant mitosis and apoptosis. *Oncogene*, **2007**, *26*, 2902-2913.
- [49] Hausmann, G.; O'Reilly, L. A.; Van Driel, R.; Beaumont, J. G.; Strasser, A.; Adams, J. M.; Huang, D. C. S. Pro-apoptotic apoptosis protease-activating factor 1 (Apaf-1) has a cytoplasmic localization distinct from Bcl-2 or Bcl-XL. *J. Cell Biol.*, **2000**, *149*, 623-633.

- [50] Kumar, B.; Kumar, A.; Pandey, B. N.; Mishra, K. P.; Hazra, B. Role of mitochondrial oxidative stress in the apoptosis induced by diospyrin diethylether in human breast carcinoma (MCF-7) cells. *Mol. Cell. Biochem.*, **2009**, *320*, 185-195.
- [51] Zhao, J.; Zhang, J.; Yu, M.; Xie, Y.; Huang, Y.; Wolff, D. W.; Abel, P. W.; Tu, Y. Mitochondrial dynamics regulates migration and invasion of breast cancer cells, *Oncogene*, **2013**, *32*, 4814-4824.
- [52] Boya, P.; Kroemer, G. Lysosomal membrane permeabilization in cell death, *Oncogene*, **2008**, *27*, 6434-6451.
- [53] Johansson, A.-C.; Appelqvist, H.; Nilsson, C.; Kagedal, K.; Roberg, K.; Oellinger, K. Regulation of apoptosis-associated lysosomal membrane permeabilization. *Apoptosis*, **2010**, *15*, 527-540.
- [54] Dai, Z.-C.; Chen, Y.-F.; Zhang, M.; Li, S.-K.; Yang, T.-T.; Shen, L.; Wang, J.-X.; Qian, S.-S.; Zhu, H.-L.; Ye, Y.-H. Synthesis and antifungal activity of 1,2,3-triazole phenylhydrazone derivatives. *Org. Biomol. Chem.*, **2015**, *13*, 477-486.
- [55] Hu, M.; Li, J.; Yao, S. Q. In situ "click" assembly of small molecule matrix metalloprotease inhibitors containing zinc-chelating groups. *Org. Lett.*, **2008**, *10*, 5529-5531.
- [56] Carreiras, M. C.; Eleuterio, A.; Dias, C.; Brito, M. A.; Brites, D.; Marco-Contelles, J.; Gomez-Sanchez, E. Synthesis and Friedlander reactions of 5-amino-4-cyano-1,3-oxazoles. *Heterocycles*, **2007**, *71*, 2249-2262.
- [57] Spencer, J.; Patel, H.; Amin, J.; Callear, S. K.; Coles, S. J.; Deadman, J. J.; Furman, C.; Mansouri, R.; Chavatte, P.; Millet, R. Microwave-mediated synthesis and manipulation of a 2-substituted-5-aminoxazole-4-carbonitrile library. *Tetrahedron Lett.*, **2012**, *53*, 1656-1659.

- [58] Lemaire, L.; Leleu-Chavain, N.; Tourteau, A.; Abdul-Sada, A.; Spencer, J.; Millet, R. A rapid route for the preparation of pyrimido[5,4-*d*]- and pyrido[3,2-*d*]oxazoles. *Tetrahedron Lett.*, **2015**, *56*, 2448-2450.
- [59] Klymchenko, A. S.; Pivovarenko, V. G.; Demchenko, A. P. Perturbation of planarity as the possible mechanism of solvent-dependent variations of fluorescence quantum yield in 2-aryl-3-hydroxychromones. *Spectrochim. Acta A Mol. Biomol. Spectrosc.*, 2003, *59A*, 787-792.
- [60] Krohn, K.; Rieger, H.; Khanbabae, K. A new synthesis of ortho-quinones by transition-metal-mediated oxygenation of phenols with tertbutylhydroperoxide and the Mimoun oxodiperoxo molybdenum complex [Mo(O₂)₂]PyHMPT. *Chem. Ber.*, **1989**, *122*, 2323-2330.
- [61] Doria, F.; Lena, A.; Bargiggia, R.; Freccero, M. Conjugation, substituent, and solvent effects on the photogeneration of quinone methides, *J. Org. Chem.*, **2016**, *81*, 3665-3673.

Highlights

- [1,2,3]Triazolo[4,5-*h*]- and [1,3]oxazolo[5,4-*h*]-[1,6]naphthyridines were synthesized.
- Potent photocytotoxicity with EC₅₀ values at nanomolar/low micromolar concentrations.
- High selectivity and photocytotoxicity indexes (SI=72-86, PTI>5000).
- Triplex excited state with exceptionally long lifetime (18.0 μ s)
- Light-induced production of ROS with mitochondrial and lysosomal involvement.